

**SCREENING 20-HETE INHIBITORS IN MICROSOMAL INCUBATES  
USING UPLC-MS/MS**

by

**Chenxiao Tang**

Bachelor of Science, Capital Medical University, 2014

Submitted to the Graduate Faculty of  
School of Pharmacy in partial fulfillment  
of the requirements for the degree of  
Master of Science

University of Pittsburgh

2016

Copyright © by Chenxiao Tang

2016

**SCREENING 20-HETE INHIBITORS IN MICROSOMAL INCUBATES USING  
UPLC-MS/MS**

Chenxiao Tang, B.S.

University of Pittsburgh, 2016

20-hydroxyecosatetraenoic acid (20-HETE) is a metabolite of arachidonic acid (AA) formed by cytochrome P450 (CYP) 4A11 and CYP4F2 in humans, with potent microvascular constriction activity. Inhibition of 20-HETE formation is neuroprotective in subarachnoid hemorrhage, cardiac arrest and thromboembolic stroke preclinical models. These findings suggest that inhibition of 20-HETE formation is a potential therapeutic strategy for neuroprotection after brain injury. At this point, a clinically relevant 20-HETE inhibitor is not available to be evaluated as a therapeutic intervention. Our goal is to identify a selective, metabolically stable, and potent 20-HETE inhibitor. Test compounds were obtained either via virtual screening against a CYP4F2 homology model or from scaffold hopping from structures of known inhibitors. Four different types of microsomes including human liver microsome (HLM), recombinant CYP4F2 (rCYP4F2), rat liver microsome (RLM) and rat kidney microsome (RKM) were used. AA was incubated in microsomes with/without compound for 20 min. 20-HETE formation rate was quantified using a validated UPLC-MS/MS assay and normalized by vehicle control group. Other eicosanoids including 15-, 12-HETEs, epoxyecosatrienoic acids (EETs),

and dihydroxyeicosatrienoic acids (DiHETs) were monitored simultaneously. Selected compounds were tested in HLM for metabolic stability over 60 minutes. Remaining amount of compound was quantified using UPLC-MS/MS and normalized to corresponding 0-min values. Among 26 compounds, compounds **10** and **26** both inhibited 20-HETE formation in a dose-dependent manner. At 2500nM, compound **10** reduced 20-HETE formation to  $19.9 \pm 1.8\%$ ,  $24.0 \pm 5.5\%$  in rCYP4F2 and HLM compared with control; compound **26** decreased 20-HETE formation to  $32.4 \pm 6.5\%$ ,  $34.8 \pm 5.1\%$  in rCYP4F2 and HLM, respectively. After structure modification, compound **19** and its hydrochloride salt compound **18** were the most potent and dose-dependently inhibited 20-HETE formation. At 2500nM, compound **19** decreased 20-HETE formation to  $4.4 \pm 0.4\%$ ,  $8.6 \pm 1.3\%$  in rCYP4F2 and HLM, respectively without inhibitory effects on 15-, 12-HETE, EETs or DiHETS formation. Compounds **10** and **19** were more stable with  $91.4 \pm 11.0\%$  and  $100.4 \pm 1.7\%$  remaining compound at 30min in HLM compared to  $35.1 \pm 5.7\%$  of 3-(4-n-butoxyphenyl)pyrazole. These results suggested that compounds **10**, **19** and **26** are potent 20-HETE formation inhibitors, compounds **10** and **19** have improved microsomal stability, and these three compounds can serve as lead compounds for further structure modifications that may lead to novel 20-HETE formation inhibitors.

**Key words:** 20-hydroxyeicosatetraenoic acid; epoxyeicosatrienoic acid; UPLC-MS/MS; microsome incubation; inhibitor

## TABLE OF CONTENT

1.0	INTRODUCTION.....	1
1.1	BRAIN INJURY IN CEREBROVASCULAR AND CARDIOVASCULAR DISEASES.....	1
1.1.1	Stroke .....	1
1.1.2	Cardiac Arrest .....	5
1.2	ARACHIDONIC ACID METABOLISM PATHWAY AND EICOSANOIDS BIOLOGICAL EFFECTS.....	8
1.2.1	Arachidonic Acid Metabolism Pathway.....	8
1.2.2	Hydroxylase Pathway and 20-HETE Biological Function.....	9
1.2.3	Epoxygenase Pathway and EETs Biological Function .....	10
1.2.4	CYP450 Enzymes and Eicosanoids in Brain.....	11
1.3	PRECLINICAL AND CLINICAL STUDIES OF EICOSANOIDS IN CEREBROVASCULAR AND CARDIOVASCULAR DISEASES .....	12
1.3.1	Eicosanoids in SAH .....	12
1.3.2	Eicosanoids in Ischemic Stroke.....	14
1.3.3	Eicosanoids in Cardiac Arrest .....	15
1.4	20-HETE FORMATION INHIBITORS AND ANTAGONISTS .....	16
1.4.1	20-HETE Formation Inhibitors .....	17
1.4.2	20-HETE Antagonists .....	19

1.5 COMPUTATIONAL CHEMISTRY .....	21
2.0 METHODS AND MATERIAL .....	25
2.1 CHEMICALS AND REAGENTS .....	25
2.2 MICROSOMAL INCUBATION ASSAY .....	26
2.2.1 AA Microsomal Incubation.....	26
2.2.2 Chromatographic Analysis of CYP Eicosanoids.....	27
2.3 MICROSOMAL STABILITY ASSAY .....	28
2.3.1 Compounds Microsomal Stability Assay .....	28
2.3.2 Chromatographic Analysis Of Compounds.....	29
2.3 STATISTICAL ANALYSIS .....	30
3.0 RESULTS .....	31
3.1 COMPOUNDS 1-15 INHIBITORY EFFECT AGAINST 20-HETE FORMATION IN HLM, RLM, RKM AND rCYP4F2.....	31
3.2 COMPOUNDS 21-26 INHIBITORY EFFECT AGAINST 20-HETE FORMATION IN HLM, RLM, RKM AND rCYP4F2.....	34
3.3 COMPOUNDS 16-19 INHIBITORY EFFECT AGAINST 20-HETE FORMATION IN HLM, RLM, RKM AND rCYP4F2.....	37
3.4 INHIBITORY EFFECT AGAINST EPOXYGENASE PATHWAY .....	40
3.5 MICROSOMAL STABILITY PROFILE OF COMPOUNDS.....	42
4.0 DISCUSSION .....	44

4.1 INTERSPECIES DIFFERENCE .....	44
4.2 EFFECT OF ORGANIC SOLVENT ON METABOLIC ACTIVITY .....	45
4.3 INDUCTION IN 20-HETE FORMATION .....	46
4.4 ENDOGENOUS OR EXOGENOUS COMPOUNDS THAT SHARE CYP4F2 METABOLISM PATHWAY .....	47
4.5 PHYSICOCHEMICAL PROPERTIES FOR DRUGGABLE COMPOUNDS .....	49
4.6 sEH INHIBITION OR 20-HETE INHIBITION .....	49
5.0 CONCLUSION .....	52
6.0 FUTURE DIRECTION .....	53
APPENDIX. ABBREVIATION .....	54
BIBLIOGRAPHY .....	56

## LIST OF TABLES

<i>Table 1. Summary of 20-HETE inhibitors .....</i>	<i>20</i>
<i>Table 2. Compounds 1-15 inhibition against 20-HETE formation in percent of control.....</i>	<i>32</i>
<i>Table 3. Compounds 21-26 inhibition against 20-HETE formation in percent of control.....</i>	<i>35</i>
<i>Table 4. Compounds 16-19 inhibition against 20-HETE formation in percent of control.....</i>	<i>38</i>



## LIST OF FIGURES

<i>Figure 1. Arachidonic acid metabolism pathway.....</i>	<i>9</i>
<i>Figure 2. Compounds 1-15 inhibition against 20-HETE formation in four different microsomes.....</i>	<i>32</i>
<i>Figure 3. Compounds 3, 7, and 10 dose-dependent inhibition against 20-HETE formation in HLM.....</i>	<i>34</i>
<i>Figure 4. Compounds 21-26 inhibitory effect against 20-HETE formation in four different microsomes.....</i>	<i>35</i>
<i>Figure 5. Compounds 25 and 26 dose-dependent inhibition against 20-HETE formation in HLM.....</i>	<i>37</i>
<i>Figure 6. Compounds 16-19 inhibitory effect against 20-HETE formation in four different microsomes.....</i>	<i>38</i>
<i>Figure 7. Compounds 18 and 19 dose-dependent inhibition against 20-HETE formation in HLM (A) and rCYP4F2 (B). .....</i>	<i>40</i>
<i>Figure 8. Compound 10 (A), compound 19 (B) and compound 26 (C) selectivity data in HLM.....</i>	<i>41</i>
<i>Figure 9. Microsomal stability profile of compound 10, 19, 26 and 3-(4-n-Butoxyphenyl)pyrazole .....</i>	<i>43</i>

## PREFACE

I am heartily thankful to my advisor, Dr. Samuel M. Poloyac, whose encouragement, guidance and support from the initial to the final stage enabled me to obtain a deeper understanding of the project. He coached me in my independent thinking skills and experiment designing skills, and provided me opportunities and excellent suggestions to present this project.

I would like to thank Dr. Lee A. McDermott for his instruction. Moreover, he also designed the novel compounds for our experiments. He is always patient answering my questions and gave me detailed and practical suggestions throughout the project.

I would like to thank Dr. David R. Koes and Somayeh Piradhi, who did the CYP4F2 homology modeling and virtual screening. I really appreciate having the opportunity to learn basic concepts in computational chemistry.

I would like to thank to all the members in Dr. Poloyac's lab: Dr. Margaret Beth Minnigh, Patrick J. Oberly, Tricia M. Miller, Kacey B. Anderson, and Lingjue Li. Without your help and encouragement, I wouldn't have been able to finish this project.

I offer my gratitude to all of those who helped me, especially Dr. Yoko Franchetti, Dr. Edward L. Berkowitz, Ziheng Hu, and Yan Zhang, in any respect during my study in School of Pharmacy and throughout the completion of the project.

Lastly, I would like to thank my family members, who supported and encouraged me to chase my dream and are always there whenever I need them.

## **1.0 INTRODUCTION**

### **1.1 BRAIN INJURY IN CEREBROVASCULAR AND CARDIOVASCULAR DISEASES**

#### **1.1.1 Stroke**

Stroke is the fifth leading cause of death in the US. Each year, approximately 795,000 people experience a new or recurrent stroke [1]. There are two types of strokes: ischemic stroke and hemorrhagic stroke. Ischemic strokes are caused by obstruction within a blood vessel that supplies blood to the brain. It accounts for 87% of all strokes [1]. Hemorrhagic strokes are less common, accounting for 13% of all stroke cases [1]. There are two types of hemorrhagic strokes based on location: intracerebral hemorrhage (ICH) and subarachnoid hemorrhage (SAH), taking up 10% and 3% of all strokes, respectively [1]. ICH happens when diseased blood vessels burst and blood leaks into brain parenchyma or the surrounding meningeal spaces. SAH refers to bleeding into the subarachnoid space between the pial and arachnoid membranes. According to the American Heart Association/American Stroke Association (AHA/ASA) website, strokes caused by unknown factors are categorized as cryptogenic stroke. Transient ischemic attack (TIA) is a transient episode of neurologic dysfunction caused by ischemia in focal brain, spinal cord, or retinal, without acute infarction. TIA symptoms occur rapidly and last for a short time, usually

less than an hour. Patients with untreated TIA have a 10% chance of developing a stroke in the next 7 days [1].

**1.1.1.1 Ischemic Stroke:** Ischemic strokes are divided into two types: thrombotic stroke and embolic stroke. In thrombotic stroke, a blood clot is formed in an artery that supplies blood to the brain. In an embolic stroke, a blood clot or other substances travel through the bloodstream to an artery in the brain. Despite different types of ischemic stroke, oxygen-rich vascular supply is compromised. Ischemia causes brain damage by oxygen or glucose depletion, energy failure and disturbance of subsequent energy-dependent processes. The extent of brain injury depends on the severity, duration and location of ischemia [2]. Depletion of cellular energy causes imbalance in ion pumps. Elevation of intracellular  $\text{Na}^+$ ,  $\text{Ca}^{2+}$  and extracellular  $\text{K}^+$  will cause cytotoxic edema [3]. With energy depletion, an excitotoxic amino acid, glutamate, is released, activating of glutamate receptors which leads to  $\text{Na}^+$ ,  $\text{Ca}^{2+}$  influx, thus exacerbating edema and toxicity [3]. Generation of oxygen-free radicals and reactive oxygen species can react with cellular components and trigger inflammation and apoptotic pathways [2]. Apoptosis is an energy consuming process, so restoration of blood flow could potentiate apoptosis [3]. Inflammation molecules, free radicals, hypoxia damage and destruction of basal lamina by matrix metalloproteinases could cause disruption of the blood brain barrier (BBB) [3]. There is increased angiogenesis in ischemic stroke within penumbra in humans. Rodent studies demonstrated the increased expression of mRNA of angiogenesis genes and angiogenic protein in ischemic area, however, it is still unclear if angiogenesis response could lead to development of functional new blood vessels and improve brain function after ischemic stroke [4].

The inner core of the cerebral vascular tissue that undergoes ischemia is hypoperfused (18–20 ml/100 g/min) and is at risk of dying within hours whereas penumbra perfused at 60 ml/100 g/min is less likely to die [2]. Early restoration of blood flow by pharmacological intervention or mechanical recanalization could salvage neurons and glia cells from the inner core as well as penumbra and reduce infarct size. However, some patients experienced reperfusion injury, fatal edema and intracranial hemorrhage, after reperfusion [5]. After reperfusion, reactive hyperemia occurs where there is an elevation of regional blood flow along with loss of cerebral autoregulation and increased BBB permeability [6]. Following postischemic hyperperfusion, a secondary hypoperfusion phase occurs, which lasts for 18 to 96 hours resulting in cerebral metabolic depression, microvascular obstruction, occlusion via swelling of endothelial cells and astrocytic end-feet, and formation of endothelial microvilli. All these contribute to increased paracellular permeability, which is associated with vasogenic edema that worsens reperfusion injury. Hillis et al. reported that reduction in volume of hypoperfused brain regions is a marker of response to treatment to improve perfusion [7]. Recombinant tissue-type plasminogen activator (rt-PA) is the only drug FDA approved for treating ischemic stroke patients via its antithrombotic effect [8]. Unfortunately, rt-PA may cause symptomatic intracranial hemorrhage and should be intravenously administered within three hours after stroke symptoms onset to achieve its benefits [9, 10].

**1.1.1.2 Subarachnoid Hemorrhage:** Eighty percent of subarachnoid hemorrhage occurs due to bleeding from cerebral aneurysm and ten percent occurs due to rupture of arteriovenous malformation. Rupture of mycotic aneurysm, angioma, neoplasm and cortical thrombosis are the other remaining causes of SAH. Approximately 30,000 people experience an aneurysmal

subarachnoid hemorrhage (aSAH) each year [11]. aSAH is associated with a significant case fatality ranging from 8% to 67% and significant morbidity among survivors [12, 13].

Early brain injury (EBI) is an emerging cause of morbidity and mortality after SAH. The definition of EBI is the immediate injury to the brain within the first 72 hours of the ictus, secondary to SAH [14]. EBI refers to the complications that happen before vasospasm and delayed cerebral ischemia (DCI) [15]. During aneurysmal rupture, intracranial pressure (ICP) increases. Possible mechanisms of ICP elevation include volume increase secondary to SAH, vasoparalysis and cerebral spinal fluid (CSF) drainage obstruction [15]. If bleeding continues and ICP remains elevated, it could induce a decrease in cerebral perfusion pressure (CPP), decrease in cerebral blood flow (CBF), as  $CPP = MAP - ICP$  and  $CBF = CPP / \text{coronary vascular resistance (CVR)}$ , and cerebral ischemia and patients could die immediately [15]. Cellular apoptosis can be activated by the increase in ICP. Neuronal apoptosis has been shown in the hippocampus and cortex in humans [16]. Apoptosis has also been linked to the development of vasospasm [15]. Prolonged and ICP-independent hypoperfusion was found in the acute phase after SAH clinically and experimentally, indicating acute vasospasm [17].

Vasospasm and delayed cerebral ischemia (DCI) that happen 3-14 days after initial hemorrhage remain to be the common causes of increased morbidity [11]. Approximately 70% of patients develop cerebral vasospasm after aSAH [18]. Cerebral vasospasm describes the narrowing of cerebral arteries that can be detected by angiography or sonography [11]. Vasospasm usually has an onset at 3 days after SAH, reaches maximum constriction on 5 to 14 days and gradually resolves at 2 to 4 weeks [11]. While cerebral vasospasm has been found to be associated with the reduction in CBF in various studies, it is also associated with reduction in cerebral perfusion but not regional perfusion. This association is supported by the fact that

hypoperfusion was seen in 46 regions but 66% of these were supplied by vessels with no significant vasospasm and some patients without vasospasm still could have hypoperfused regions in a SAH cohort study [19]. DCI happens in about 30% of aSAH patients [11]. DCI is defined as the presence of focal neurological deficit or a decrease in the Glasgow Coma Scale of at least two points with an disturbance in cerebral blood flow [20]. It has long been implicated that cerebral vasospasm plays a causative role in developing DCI. However, clinical trials showed that clazosentan treatment didn't significantly reduce delayed ischemic neurological deficit while showing reduction in moderate or severe vasospasm [21]. Similarly, one parallel study found that delayed cerebral infarction could develop in brain regions without vasospasm and it accounts for >25% of infarct from DCI [22]. These indicated an association instead of a causal relationship between cerebral vasospasm and DCI, other processes that happen in a microvascular level could attribute to part of the burden from DCI [22].

Prophylactic oral nimodipine and initiation of triple-H therapy have the strongest evidence in treating vasospasm [23]. Triple-H therapy increases cerebral blood flow by increments of intravascular volume and reduction of blood viscosity, but failed to show improvement in delayed neurological deficits or clinical outcome [23]. Nimodipine is a calcium channel blocker indicated for improving neurological outcomes after SAH. In a British Aneurysm Nimodipine Trial, patients who had oral nimodipine demonstrated a 34% reduction in cerebral infarction and a 40% reduction in poor outcome at three months.

### **1.1.2 Cardiac Arrest**

Cardiac arrest is defined as the cessation of cardiac mechanical activity and confirmed by the absence of signs of circulation. In 2014, 6328 children (<18 years) and 320157 adults



experienced out-of hospital cardiac arrest and survival to hospital discharge was only around 7-10% [24]. Whole-body ischemia during cardiac arrest and after return of spontaneous circulation (ROSC) lead to a series of post-cardiac arrest syndrome, including post-cardiac arrest brain injury, post-cardiac arrest myocardial injury, systemic ischemia/reperfusion response and persistent precipitating pathology. Brain, particularly cerebral cortex, is vulnerable to ischemic/reperfusion injury and post-resuscitation neurological dysfunction of cardiac arrest represents the major cause of mortality and morbidity [25]. Upon cessation of cerebral circulation, oxygen is depleted, followed by energy depletion. Inability to maintain  $\text{Ca}^{2+}$  homeostasis could result in the release of free fatty acid, mainly arachidonic acid, and induce vasospasm. Free radical formation and activation of protease cascades lead to damage in membrane structure, DNA and mitochondria. Activation of cell-death signaling pathways and excitotoxicity during ischemia and after reperfusion of cardiac arrest all contribute to post-cardiac arrest brain injury [25-27].

Animal studies show that there is a short period of multifocal no-reflow right after resuscitation from cardiac arrest. This is followed by a 15-30 min transient global hyperemia that causes impaired cerebral autoregulation. While the cerebral metabolic fate gradually recovers, cerebral blood flow is severely reduced for 2-12 hours, which is called the delayed hypoperfusion phase. After restoration of CBF and metabolism, there might be secondary hyperemia [25, 28]. The prolonged phase of hypoperfusion is correlated to neurocognitive, behavioral, sensory and motor function deficit and may represent a therapeutic target for ischemic/reperfusion injury [16]. For example, simultaneous chest compression cardiopulmonary resuscitation (CPR) combined with abdominal binding improves cerebral perfusion by elevating cerebral perfusion pressure in dog after cardiac arrest [29]. In a ventricular fibrillation cardiac

arrest (VFCA) model in pig, the endothelin-1 treated group showed dose-dependent elevation in CBF after resuscitation from VFCA and increased resuscitation success [30]. On the contrary, BQ123, an antagonist of endothelin type A receptor, reversed cerebral hypoperfusion and improved functional outcome in cardiac arrest rats [31].

One important treatment to prevent secondary brain injury and improve neurological outcome is the application of therapeutic hypothermia. Preclinical research showed hypothermia improved functional, neurological and morphological cerebral outcome in dogs and rats [32-35]. Clinical evidence showed that 49% of the patients treated with hypothermia (33 °C) had a good outcome compared to 26% in the normothermia group, with an odds ratio of 5.25 [36]. Based on the published evidence, AHA recommended therapeutic hypothermia as standard of care in patients after resuscitation from VFCA. In 2009, an international conference provided consensus recommendations to targeted temperature management in critical care, where “therapeutic hypothermia” was recommended to replace by “targeted temperature management” and targeted temperature management profile should be explicitly indicated instead of using “mild”. Recommendations also include 32-34 °C as preferred treatment for out-of-hospital cardiac arrest adult patients with ventricular fibrillation or pulseless ventricular tachycardia and still unconscious after restoration of spontaneous circulation [37]. Possible protective mechanisms of hypothermia include: (1) a 6% reduction in cerebral metabolic rate for oxygen when every 1 °C reduction in brain temperature; (2) suppression of free radical production, excitatory amino acid release, and calcium shifts that are associated with hyperthermia; (3) attenuation of pro-apoptosis signals; (4) upregulation of p53 that promote repair after focal ischemia and (5) reduction in a neuron death marker enolase [38].

Collectively, cardiac arrest, ischemic stroke and subarachnoid hemorrhage share common mechanisms in pathophysiology of brain injury. Cerebral hypoperfusion is one common mechanism that contributes to secondary brain injury and may serve as a potential treatment target in cardiovascular and cerebrovascular diseases. 20-HETE as microvascular constrictor could also regulate CBF through alteration of CVR. The following section will introduce 20-HETE production and its biological effects.

## **1.2 ARACHIDONIC ACID METABOLISM PATHWAY AND EICOSANOIDS**

### **BIOLOGICAL EFFECTS**

#### **1.2.1 Arachidonic Acid Metabolism Pathway**

Arachidonic acid (AA) is a polyunsaturated  $\omega$ -6 fatty acid that is esterified in the cell membrane. It can be activated by cytosolic phospholipid A<sub>2</sub> (cPLA<sub>2</sub>) under different stimuli to release free AA for oxidized metabolism [39]. Once released, free AA is metabolized by three enzymatic pathways, including cyclooxygenase (COX), lipoxygenase (LOX) and cytochrome P450 (CYP450) [40]. COX catalyze AA into prostaglandins PGG<sub>2</sub> and PGH<sub>2</sub>, which are further converted into vasodilatory prostaglandins PGE<sub>2</sub>, PGF<sub>2 $\alpha$</sub> , prostacyclins PGI<sub>2</sub> and thromboxanes TXA<sub>2</sub> and TXB<sub>2</sub> [41]. Several different LOX, 5-, 12-, and 15-LOX metabolize AA into 5-, 12-, 15-HETE, which are converted to leukotrienes and lipoxins [41]. CYP450 pathways metabolize AA by hydroxylation, olefin epoxidation and bis-allylic oxidation into hydroxyeicosatetraenoic acids (HETEs) and epoxyeicosatrienoic acids (EETs). AA  $\omega$ -/ $\omega$ -1 hydroxylation happens at or

near the terminal carbon and yields 16-, 17-, 18-, 19-, 20-HETE [42]. Bis-allylic oxidation generates 5-, 8-, 9-, 11-, 12-, 13-, and 15-HETE [42, 43]. Olefin oxidation provides four EETs: 5,6-, 8,9-, 11,12-, and 14,15-EET [42]. A study done in a group of human recombinant enzymes showed that CYP2C19 had the highest catalytic activity (32 pmol/ pmol P450/ min) to metabolize AA, followed by CYP1A1, 4F3B, 4A11 and 4F2 [44]. **Figure 1** depicts three pathways of AA metabolism.

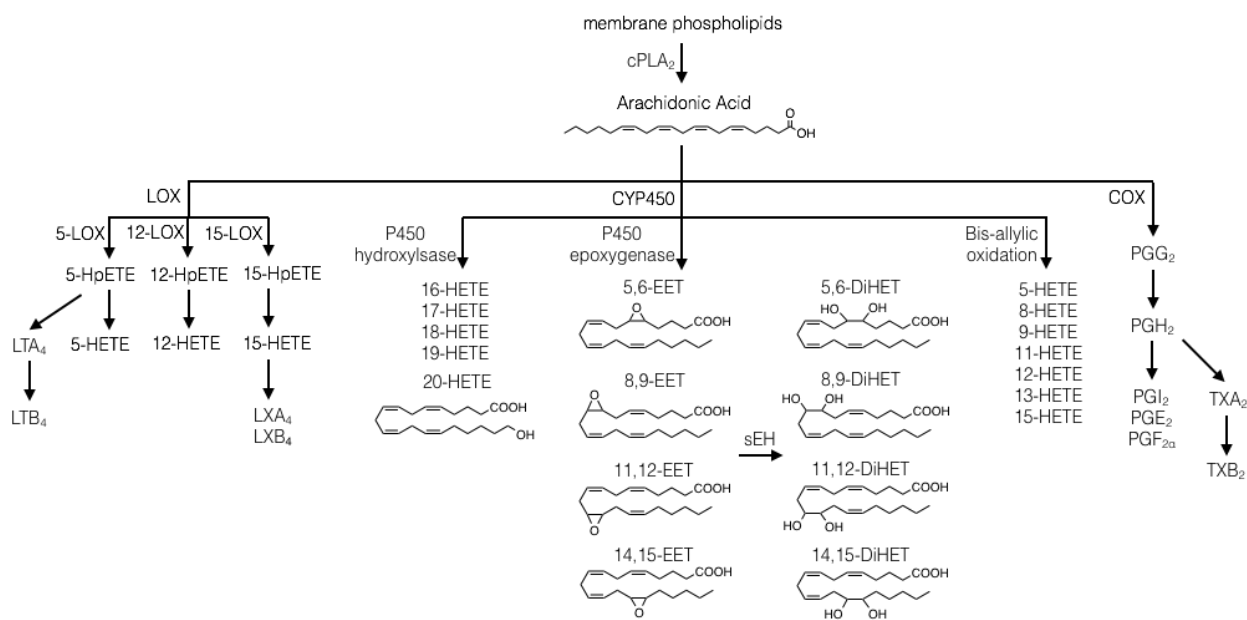


**Figure 1. Arachidonic acid metabolism pathway**

### 1.2.2 Hydroxylase Pathway and 20-HETE Biological Function

CYP450 hydroxylase pathway regulates formation of 16-, 17-, 18-, 19-, and 20-HETE [42]. 20-HETE is the major metabolite of AA in various organs such as liver, kidney, heart, lung and cerebral arteries [40, 45, 46]. CYP4A and 4F subfamilies are responsible for ω-hydroxylation of AA to form 20-HETE [40]. Powell et al. showed that CYP4A11, 4F2 produced 20-HETE in

human liver and kidney microsomes, and Lasker et al. demonstrated that CYP4F2 was responsible for predominant 20-HETE formation in human kidney [47, 48]. Incubation with human recombinant CYP4F3B exhibited high catalytic hydroxylation of AA, and AA  $\omega$ -hydroxylated metabolites formed by CYP4F3B decreased to 8% when DHA (50  $\mu$ M) was present, which indicates CYP4F3B is an isoform that could also form 20-HETE [49, 50]. A non-CYP4 isoform CYP2U1, localized in human brain tissue, also converted AA into 19-HETE and 20-HETE [51]. In rat, CYP4A1, 4A2, 4A3, 4A8, 4F1, 4F4 has been shown to generate 20-HETE and CYP4A2 is considered the major isoform for 20-HETE formation [52-56]. 20-HETE has potent microvascular constriction effects, constricting renal, cerebral, mesenteric and skeleton muscle arterioles [40]. 20-HETE inhibits large conductance  $Ca^{2+}$ -activated  $K^+$  ( $K_{Ca}$ ) channels, leading to depolarization of membrane potential and vasoconstriction [57]. 20-HETE is also involved in myogenic response in renal, cerebral, mesenteric and skeleton muscle, autoregulation of renal and cerebral blood flow, ischemia-induced angiogenesis and PPAR-mediated inflammation [57-60].

### **1.2.3 Epoxygenase Pathway and EETs Biological Function**

CYP450 epoxygenase pathway generates four EETs: 5,6-EET, 8,9-EET, 11,12-EET and 14,15-EET [61]. In general, CYP1A, 2B, 2C, 2D, 2G, 2J, 2N can generate these metabolites from AA [39, 62]. In livers and kidneys of both humans and rats, CYP2C8, 2C9 are the major isoforms for EETs formation [39]. CYP2J2 is the predominant isoform for EETs formation in human and rat heart [63]. Once formed, the majority of EETs are esterified to cellular glycerophospholipids [39]. EETs can be metabolized by soluble epoxide hydrolase (sEH) localized in liver, kidney,

and brain into corresponding DiHETs [39, 64]. DiHETs are generally viewed as biologically inactive or less effective compared with EETs [39, 65]. Other metabolism pathways of EETs include  $\beta$ -oxidation, CYP metabolism and glutathione conjugation. On the contrary to 20-HETE, EETs dilate kidney, cerebral, mesenteric and pulmonary arterioles, inhibit T-type calcium channels, and activate large conductance  $\text{Ca}^{2+}$ -activated  $\text{K}^+$  ( $\text{K}_{\text{Ca}}$ ) channels, leading to hyperpolarization of membrane potential and vasodilation [40, 65, 66]. EETs have anti-inflammatory effects and inhibit platelet aggregation [40]. EETs also stimulate angiogenesis by involving MAPK, P13-k/Akt signaling pathway and eNOS pathway [67].

#### **1.2.4 CYP450 Enzymes and Eicosanoids in Brain**

CYP2C, 2D, 2J, 4A, 4F subfamilies are expressed in brain [40, 68, 69]. 20-HETE and EETs are formed when incubated with AA in rat cerebral arteriole microsomes and can be found in human CSF [58, 70]. 20-HETE is produced in vascular smooth muscle cells, vascular endothelium and astrocytes, while EETs are produced in neurons, astrocytes and endothelial cells [40, 71, 72]. sEH that bioinactivate EETs is expressed in smooth muscles of the arterioles, neuronal cell bodies, oligodendrocytes, and astrocytes [73]. As discussed above, 20-HETE and EETs have opposite effects on cerebral arteries. 20-HETE constricts cerebral arteries by activating PKC, Ras, tyrosine kinase, MAP and rho kinase pathways, depolarize cell membrane by blocking  $\text{K}_{\text{Ca}}$  channels, and activating L-type  $\text{Ca}^{2+}$  channels [74]. 20-HETE and EETs regulate basal blood flow in cerebral microcirculation. Subdural administration of CYP450 epoxygenase inhibitor miconazole induced a 29.7% decrease in basal blood flow [75]. At  $10^{-6}$  mol/L, 20-HETE decreased basal cerebral arteries diameters by 25.3% [58]. 20-HETE has a potential role in CBF

autoregulation and this is supported by the evidence that 20-HETE concentration levels increased six times as transmural pressure elevated from 20 to 140 mm Hg and *in vivo* inhibition of 20-HETE alleviated autoregulation of CBF to elevation of arterial pressure [58]. EETs dilate cerebral arteries by activating  $K_{ca}$  channels and hyperpolarize cell membranes. 5,6-EET and 14,15-EET were identified when blood-free mouse brain slices were incubated with exogenous radiolabeled AA [76]. Topical application of brain-synthesized 5,6-EET or synthetic 8,9-EET (5  $\mu$ g/ml) showed a 28% and 8% dilation in cerebral arteriolar, respectively [76]. Co-localization of CYP2C11 and sEH at extrinsic parasympathetic and sensory vasodilator fibers suggested that EETs have a role in neurogenic control of cerebral arteries [77]. EETs have also been demonstrated to be key mediators in neurovascular coupling [64].

### **1.3 PRECLINICAL AND CLINICAL STUDIES OF EICOSANOIDS IN CEREBROVASCULAR AND CARDIOVASCULAR DISEASES**

Multiple animal and clinical studies have demonstrated that upregulation of 20-HETE is detrimental, whereas inhibition of 20-HETE produces protective effects in CA, SAH and ischemic stroke.

#### **1.3.1 Eicosanoids in SAH**

A number of studies have investigated the role of 20-HETE and EETs in SAH. Various studies proved that inhibition of 20-HETE had beneficial effects in CBF and neurological outcomes.

Kehl et al. showed that 20-HETE levels drastically increased from 12 to 199 ng/ml in vehicle-treated rat after SAH [78]. Rats pretreated with N-hydroxy-N-(4-butyl-2-methylphenyl)formamide (HET0016 10mg/kg i.v.), a 20-HETE formation inhibitor, significantly reduced the initial fall in CBF at 10 min after induction of SAH [78]. Pretreatment of N-(3-chloro-4-morpholin-4-yl) phenyl-N'-hydroxyimido formamide (TS-011 0.01–0.1 mg/kg i.v.), another 20-HETE formation inhibitor, prevented sustained fall in CBF in rat after induction of SAH [78, 79]. In a dual-hemorrhage model of SAH in rat, rats that received TS-011 (0.1 mg/kg i.v.) showed recovery of cerebral artery diameter, CBF returned to control values, and reversion of delayed vasospasm [80]. Eicosanoids can be found in human CSF as well [70, 81]. Our laboratory found in aSAH patients CSF 20-HETE concentrations was associated with delayed cerebral ischemia (DCI) and Hunt & Hess score, which represents severity of hemorrhage [82]. This is the first clinical evidence that supports an association between 20-HETE CSF levels with poorer aSAH outcome. Along with the increase of 20-HETE, CSF levels of the protective vasodilator 14,15-EET also increased in aSAH patients who experienced DCI [83]. Our laboratory also found that aSAH patients with moderate or high 20-HETE CSF concentrations were more likely to have unfavorable 3 and 12-months Modified Rankin Scale, quicker onset to develop clinical neurologic deterioration and three-fold higher 3 and 12-month mortality [84].

Decreasing EETs bioinactivation through sEH gene deletion is another strategy to produce protective effects after SAH. The most common genetic variants for EPHX2, a gene that regulates sEH transcription, are K55R and R287Q. K55R variant confers the increase of sEH activity and lowers EETs levels, while R287Q variant leads to a decrease in sEH activity and higher EETs levels. aSAH patients with K55R variants had higher odds of new stroke, higher



mortality, and worse ICU discharge [85]. In sEH knockout mice, cerebral edema and vascular inflammation was less, and behavioral outcome was better compared with wild type mice [86].

### **1.3.2 Eicosanoids in Ischemic Stroke**

Multiple studies in ischemic stroke models established that an increase in 20-HETE is deleterious, and an increase in EETs is favorable. Direct infusion of 20-HETE (8 mg/kg or 12 mg/kg) into carotid artery induced severe neurological deficit and large cortical infarcts that resembled the infarct in transient ischemic stroke model in rat [79]. After temporal focal ischemia in rats, HET0016 (10 mg/kg i.p.) administration is associated with 79.6% reduction in 20-HETE levels in brain cortical tissue [87]. HET0016 treated group exhibited reduced lesion volume and attenuation of decreased CBF [87]. Similarly, in ischemic stroke rat model, brain 20-HETE levels significantly increased within 5.5 h after transient middle cerebral artery occlusion (MCAO) [88]. Treatment with TS-011 (0.3 mg/kg) led to smaller infarct volume, and improved neurological and functional outcome compared with vehicle treatment [88]. 20-HETE is found in plasma of ischemic stroke patients, and is associated with unfavorable outcome. In acute ischemic stroke patients, plasma 20-HETE as well as EETs, DiHETs, and F2-isoprostane levels significantly increased compared with healthy controls, and 20-HETE and EETs levels attenuated at 30 days post ischemic stroke [89]. 20-HETE concentrations are associated with greater neurological impairment, reduced modified barthel index (MBI), and reduced cognitive function.

Increasing EETs by inhibiting sEH is another strategy to produce protective effect after ischemic stroke. Acute inhibition of sEH by trans-4-[4-(3-adamantan-1-yl-ureido)-

cyclohexyloxy]-benzoic acid (t-AUCB) increased EETs to DiHETs ratio by two fold in rat brain cortex [90]. t-AUCB reduced cortical infarct volume by 35%, decreased neuronal cell death and improved functional outcome [90]. sEH knock-out reproductively senescent female mice subjected to MCAO showed decreased infarct size and increased cerebral perfusion at 24 h after MCAO [91]. Interestingly, therapeutic ultrasound has shown beneficial effect in stroke patients by ultrasound-mediated thrombolysis through augmenting vasodilator eicosanoids 8,9-EET, 11,12-EET, 14,15-EET by more than two fold [92].

### **1.3.3 Eicosanoids in Cardiac Arrest**

20-HETE and EETs disturbance were also found in CA. In an asphyxia cardiac arrest model performed in our laboratory, 16-18 day old pediatric rats underwent 9 min /12 min (moderate /severe) cardiac arrest. After moderate cardiac arrest, 8,9-EET and 14,15-EET significantly increased in cortex and subcortical region. After severe cardiac arrest, 20-HETE significantly increased in cortex and subcortical regions [93]. HET0016 (0.9 mg/kg i.v.) administration inhibited 20-HETE formation, improved cortical perfusion, decreased neurological deficit score (NDS), reduced pyknotic neurons, and percentage of brain tissue water [93]. This suggests that inhibition of 20-HETE improves CBF and reduces neurodegeneration. Early administration of HET0016 (1 mg/kg) plus delayed therapeutic hypothermia (34 °C) in neonatal piglets after hypoxia-ischemia enhanced the benefit of delayed therapeutic hypothermia in neuron protection, HET0016 plus delayed therapeutic hypothermia treated group showed increase in viable neurons in putamen, somatosensory cortex and ventral posterolateral nucleus thalamus [94].

There is inconsistency regarding the protective effects of sEH pharmacological inhibition or gene deletion. Hutchens et al. showed that sEH gene deletion mice subjected to 10 min CA had significantly lower survival rate than wild type mice at 10 min and 24 h after CA and they required significantly longer CPR time and more epinephrine [95]. Other studies supported the favorable effect of sEH gene deletion or pharmacological inhibition. For example, sEH inhibition by 4-phenylchalcone oxide (4-PCO) in mouse CA/CPR model had reduced neuronal cell death and improved memory function by inducing anti-inflammatory and neuroprotective IL-10 expression [96].

Together, these studies suggest that reducing 20-HETE production may serve as a potential therapeutic strategy in cerebrovascular and cardiovascular diseases. Inhibiting 20-HETE formation or blocking 20-HETE action can diminish vasoconstriction thus increasing cerebral blood flow and produce beneficial neurological outcome.

#### **1.4 20-HETE FORMATION INHIBITORS AND ANTAGONISTS**

According to the AHA/ASA stroke guidelines, blood pressure management for ischemic stroke treatment is a class I recommendation, where treating peri-infarct penumbra characterized with impaired cerebral blood flow is dependent on mean arterial blood pressure [8, 97]. The only drug that is FDA approved for ischemic stroke treatment is recombinant tissue-type plasminogen activator (rt-PA) to dissolve clots and restore cerebral blood flow [8]. Unfortunately, rt-PA may cause symptomatic intracranial hemorrhage and must be administered early after strokes [9]. For aSAH patients, antifibrinolytic treatment following prophylaxis against vasospasm is

recommended by AHA/ASA aSAH guidelines to reduce the threat of ischemic neuronal damage through controlling intracranial pressure, decreasing the metabolic rate of oxygen use, and improving CBF [98]. However, few therapeutic treatments exist for SAH-induced brain injury [98]. In 2010 CA guidelines, neurocritical care was emphasized for post-cardiac arrest patients. Few neuroprotective drugs have been tested in clinical trials and no pharmacological agents were observed to have neuroprotective effect [59]. Thus, intervention treatment for post-injury cerebral hypoperfusion and CBF disturbance is inadequate. Emerging evidence of 20-HETE as pathogenesis in various neurovascular diseases and its association with unfavorable outcomes has made it a potential treatment target in ischemic stroke, SAH and CA.

#### **1.4.1 20-HETE Formation Inhibitors**

There has been a wealth of compounds synthesized to either target enzymes that are responsible for 20-HETE formation or act as antagonists of 20-HETE to block its effects. **Table 1** is a summary of IC<sub>50</sub> values and inhibition mechanisms of 20-HETE inhibitors and antagonists [99]. Several compounds inhibit 20-HETE and EETS formation nonselectively.  $\beta$ -diethylaminoethyldiphenylpropylacetate (SKF-525A) nonselectively inhibits EETs and 20-HETE formation by binding to the heme in CYP enzymes and reduces availability of the heme to incorporate into CYP enzymes [40, 100]. 17-octadecynoic acid (17-ODYA) is a fatty acid analogue, which inhibits 20-HETE formation avidly depending on the terminal acetylenic moiety [101]. However, it also inhibits epoxygenases effectively at the same concentration [102]. Compound 1-aminobenzotriazole (ABT) (50 mg/kg) administered intraperitoneally completely inhibited 20-HETE and EETs formation, it disrupts CYP450 function by binding a benzene

group to the heme [103, 104]. In addition to these compounds, endogenous vasodilators, nitric oxide (NO) and carbon monoxide (CO), bind to the heme in the CYP enzymes and block 20-HETE and EETs formation simultaneously even though NO donor dose-dependently inhibited 20-HETE formation in renal microsomes [105].

Selective 20-HETE formation inhibitors were developed to specifically target the hydroxylase pathway, while minimizing the effects on the epoxygenase pathway. N-methylsulfonyl-12,12-dibromododec-11-enamide (DDMS) and 12-12-dibromododec-11-enoic acid (DBDD) are dibromoolefinic fatty acids [106]. In rat renal cortical microsomes, DDMS and DBDD inhibited  $\omega$ -hydroxylation of AA with  $IC_{50}$  of 2  $\mu$ M and there was about a 20% reduction in EETs at 10  $\mu$ M. As concentration increases, DDMS and DBDD inhibit the epoxygenase pathway with an  $IC_{50}$  of 60  $\mu$ M and 51  $\mu$ M, respectively [106]. One-hour intravenous infusion of DDMS (10 mg/kg) reduced rat renal 20-HETE formation by 70% [107]. Because DDMS and DBDD are fatty acids, in vivo application might be restrained due to protein binding [40]. HET0016 is a selective, potent 20-HETE formation inhibitor in both humans and rats. It inhibits 20-HETE in a dose-dependent manner with an  $IC_{50}$  value of  $35.2 \pm 4.4$  nM and  $8.9 \pm 2.7$  nM in rat and human renal microsomes, respectively [108]. EETs inhibition occurs at  $IC_{50}$  ( $2800 \pm 300$  nM) 100 times higher [108]. However, HET0016 is plagued by low water solubility (3.7  $\mu$ g/ml), short half-life ( $39.6 \pm 20.0$  min) and instability under acidic environment (43.2% remaining) [109, 110]. Several pyrazole and isoxazole derivatives of HET0016 showed selective inhibition against 20-HETE formation with better stability and solubility profile, such as 3-(4-n-Butoxyphenyl)pyrazole [110]. N-(3-chloro-4-morpholin-4-yl) phenyl-N'-hydroxyimidoformamide (TS-011) is a newer selective, potent 20-HETE formation inhibitor with a  $IC_{50}$  range of 10-50 nM in human renal microsomes and recombinant CYP4A11, 4F2, 4F3B against 20-

HETE formation and has little effect against other CYP450 isoforms [79]. Unfortunately, TS-011 has a shockingly short half-life of 10 min when i.v. injected in rat and its main metabolite did not show inhibitory effects against 20-HETE formation in human renal microsomes [79].

Several clinically approved drugs and supplements have demonstrated inhibitory effects against 20-HETE formation. Fluoxetine has been proven to have protective effects by preventing BBB disruption in global ischemia-induced neuronal death [111]. In a study done in neonatal rats, transient postnatal fluoxetine (10 mg/kg) exposure reduced brain 20-HETE concentration by 70.3%, indicating that fluoxetine may be a potential therapeutic agent in ischemic brain injury patients [112]. Isoniazid inhibited 20-HETE levels in rat liver and kidney tissue by  $34\pm 10\%$  and  $15.6\pm 5.3\%$  of control, respectively [113]. Cardiac hypertrophy-induced rats treated with isoniazid (200mg/kg/day) showed increased cardiac 19-HETE levels by 20-fold and significant reduced 20-HETE levels by 98% [114]. By Monte Carlo simulations, El-Sherbeni et al. predicted that 2.5g daily high and safe oral resveratrol will decrease 20-HETE levels by 16-35% in 90% of human population [44]. Sesamin and sesamol are plant lignans derived from sesame, which inhibited 20-HETE formation both *in vitro* and *in vivo*, while inhibiting epoxygenase activity with an  $IC_{50}$  value of 50  $\mu$ M [115].

#### **1.4.2 20-HETE Antagonists**

Several 20-HETE analogues have shown to antagonize 20-HETE activity in renal and cerebral arteries, such as 5-, 15-, 19-HETE and 20-hydroxyeicosa-6(Z),15(Z)-dienoic acid (6(Z),15(Z)-20-HEDE) [40]. 2,5,8,11,14,17-hexaoxonadecan-19-yl 20-hydroxyeicosa-

6(Z),15(Z)-dienoate (20-SOLA) is a novel, water soluble, 20-HETE antagonist that has shown to be able to reduce blood pressure in cyp4a14 knockout mice [116].

**Table 1. Summary of 20-HETE inhibitors**

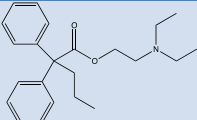
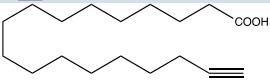
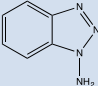
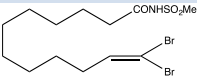
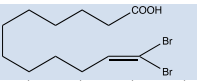
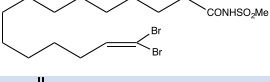
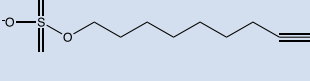
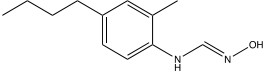
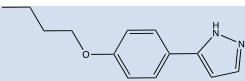
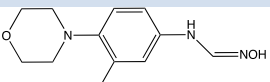
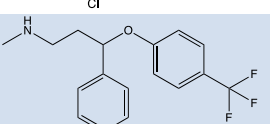
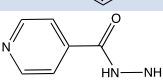
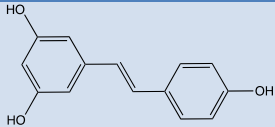
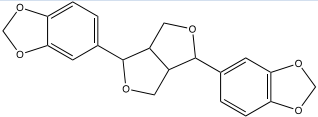
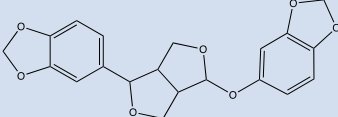
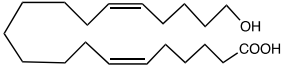
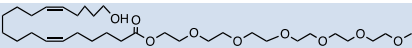
Name	Structure	IC <sub>50</sub> for 20-HETE formation in renal microsomes	Type of inhibitor	Reference
SKF-525A		Unknown	Mechanism-based	[40, 100, 117]
17-ODYA		<100 nM (rat)	Mechanism-based	[99, 102, 118]
ABT		μM range	Mechanism-based	[118, 119]
DDMS		2 μM (rat)	Mechanism-based, Reversible	[106, 107]
DBDD		2 μM (rat)	Reversible	[106]
DPMS		31 μM (rat)	Unknown	[106]
10-SUYS		10.1±2.6 μM (rat)	Mechanism-based	[120, 121]
HET0016		8.9±2.7 nM (human) 35.2±4.4 nM (rat)	Unknown	[99, 108]
3-(4-n-Butoxyphenyl)pyrazole		23±12 nM (human)	Unknown	[110]
TS-011		8.42 nM (human) 9.19 nM (rat)	Unknown	[79]
Fluoxetine		Unknown	Alter CYP4A expression	[112, 122]
Isoniazid		Unknown	Alter CYP4A expression	[113, 114]

Table 1 (continued)

Resveratrol		3 $\mu$ M (human liver microsomes)	Time-dependent inhibition against CYP1A1, alter CYP4A expression	[44, 123, 124]
Sesamin		5.3 $\mu$ M (human)	Unknown	[115]
Sesamolin		3.4 $\mu$ M (human)	Unknown	[115]
6(Z),15(Z)-20-HEDE		Unknown	Antagonist	[40]
20-SOLA		Unknown	Antagonist	[116]

## 1.5 COMPUTATIONAL CHEMISTRY

Protein structures can be ascertained by X-ray crystallography, NMR spectroscopy or electron microscopy. Protein crystallization is to crystallize protein to obtain its 3D structure, which can aid in *in silico* drug design. Crystallizing membrane-bound proteins has many barriers including: (1) extraction only takes place when detergents in presence due to the hydrophobicity of protein surfaces; (2) difficulty in purifying membrane proteins because of their instability once solubilized in detergents and (3) generating low yield from purified proteins to high-resolution structure [125]. In addition to the challenges of protein crystallization, the methods used for determining their structures also have their drawbacks. X-ray crystallography and NMR spectroscopy have disadvantages when membrane proteins are embedded in a lipid bilayer [126]. The only way to determine structure of membrane-bound protein in its membrane context is by



using electron crystallography. This technique is not widely used because producing two-dimensional crystals that diffract to high-resolution requires sufficient amount of stable and compatible membrane proteins [125].

When a protein 3D structure is not available, homology modeling can help in constructing a 3D model of target protein and structure-based drug design [127]. Homology modeling, also known as comparative modeling, allows construction of 3D structure of target protein based on its amino acid sequence and templates of experimental 3D structures that are evolutionarily related to the target protein [128].

The first step of homology modeling is to select the most appropriate template among available protein structures for target sequence. Templates can be found in databases like Protein Data Bank, CATH, MODBASE, SCOP and etc. [129]. BLAST server provides a comparison of the target sequence with a library of protein sequences and outputs a list of 3D protein structures based on the sequence identity [130]. The second step is to align the target sequence with the template, which is the basis for homology modeling. There are several methods that can achieve target-template alignment, including PSI-BLAST, SALIGN, SAM-T02 and etc. [129]. In some alignments, using multiple template structures and sequence information is beneficial [131]. For example, human CYP4F11 and CYP4F3A were aligned using mammalian CYP2C5 bound to 3-dimethylsulfaphenazole, CYPBM3 (2HPD), CYPterp (1CPT), CYPcam (2CPP), and CYPeryF (1OXA) as structural templates [132]. If the sequence homology between target protein and protein template is larger than 50%, then the template protein structure will be a general good model. However, if the homology drops to 20%, there will be large structural differences [133]. After the alignment of a target sequence with the template sequence, the next step is to build and refine the 3D structural model of the target protein. The model should include building of the

backbone of the protein, loops and side-chains [134]. Several programs can carry out model building. The SWISS-MODEL models by the rigid-body assembly method, where rigid bodies derived from the core of the aligned regions are used to construct a model [129, 135]. The SegMOD program employs modeling by segment matching, where atomic positions obtained from the alignment were used to find resembling segments [135, 136]. The third method is to model based on satisfaction of spatial restraint, which can be achieved by the MODELLER program [137]. The newest homology modeling method, artificial evolution, can be done by the NEST program, which employs the structural evolution from the template to the target protein [138, 139]. Homology modeling is a iterative process and needs model optimization which can be applied by molecular mechanics force field, molecular dynamics, Monte Carlo and genetic algorithm-based sampling [134]. Lastly, the homology model needs to be validated by determining if the model has the correct fold, similarity between the target and template sequences, stereochemistry of the model and model structure in the functional environment [134].

Homology modeling can be used together with virtual screening to help identify novel compounds. Virtual screening enables identification of biologically active molecules that bind to the protein target [140]. When target information is available we can use structure-based virtual screening. In other cases, when this information is not available, ligand-based virtual screening can be used [141]. For example, two retinoic acid receptor (RAR) agonists with an  $IC_{50}$  value of 50 nM were identified based on virtual screening from Available Chemicals Directory using a RAR- $\alpha$  model. One of the compounds displayed novel structural features that may assist in the development of novel ligands for cancer therapy [142]. Pharmacophore modeling is a major tool in ligand-based virtual screening in drug discovery. According to IUPAC, a pharmacophore model is an ensemble of steric and electronic features that is necessary to ensure the optimal

supramolecular interactions with a specific biological target and to trigger (or block) its biological response [143]. Pharmacophore modeling can be improved by ligand-based or structure-based methods [144]. For example, 22 structure-based and 3 ligand-based pharmacophore models identified 58 compounds that were potential sEH inhibitors. Among 48 tested compounds, 19 were sEH inhibitors with  $IC_{50} < 10 \mu M$ , one was the most potent with an  $IC_{50}$  of 4.2 nM [145].

Human CYP4 family consists of 13 isozymes [99]. There is an ester bond between the heme 5-methyl group and a glutamic acid, which is conserved in the CYP4 family [146]. The sequence and structure of CYP4F2 is closely related to other isoforms in the CYP4F subfamily. CYP4F2 and CYP4F3B have high similarity in their amino acid sequences; they have more than 93% sequence identity [147]. CYP4F11 has 80.0% and 82.3% sequence identity with CYP4F2 and CYP4F3, respectively [148]. Thus, predicting the 3D structure of CYP4F2 using homology modeling and virtual screening against compound libraries could assist in discovery of novel selective and potent enzyme inhibitors.

CYP450-derived eicosanoids have a wide range of biological functions and the alteration of eicosanoid levels is associated with pathophysiological conditions in CA, SAH and ischemic stroke. Since 20-HETE is a potent microvascular vasoconstrictor that plays a role in CBF autoregulation and cerebralvascular tone, CYP4A and CYP4F subfamilies that are involved in 20-HETE formation may be potential therapeutic targets in these diseases. Consequently, development of enzyme inhibitors that target the CYP4F2 isoform should be studied profoundly to aid in the study of vasoactive metabolites pathophysiological roles. The goal of this research project is to identify novel, potent, selective, metabolically stable 20-HETE formation inhibitors with improved solubility and better BBB permeability.

## 2.0 METHODS AND MATERIALS

### 2.1 CHEMICALS AND REAGENTS

Test compounds **1-19** were obtained from a proprietary library available to our laboratory; test compounds **21-26** were obtained via virtual screening from NCI database against a CYP4F2 homology model. Stock standards of (±)5,6-dihydroxy-8Z,11Z,14Z-eicosatrienoic acid (5,6-DiHET), (±)8,9-dihydroxy-5Z,8Z,14Z-eicosatrienoic acid (8,9-DiHET), (±)11,12-dihydroxy-5Z,8Z,14Z-eicosatrienoic acid (11,12-DiHET), (±)14,15-dihydroxy-5Z,8Z,11Z-eicosatrienoic acid (14,15-DiHET), (±)8(9)-epoxy-5Z,11Z,14Z-eicosatrienoic acid (8,9-EET), (±)11(12)-epoxy-5Z,8Z,14Z-eicosatrienoic acid (11,12-EET), (±)14(15)-epoxy-5Z,8Z,11Z-eicosatrienoic acid (14,15-EET), 20-hydroxy-5Z,8Z,11Z,14Z-eicosatetraenoic acid (20-HETE), 20-hydroxy-5Z,8Z,11Z,14Z-eicosatetraenoic-16,16,17,17,18,18-d<sub>6</sub> acid (20-HETE-d<sub>6</sub>), 12S-hydroxy-5Z,8Z,10E,14Z-eicosatetraenoic acid (12-HETE), 15S-hydroxy-5Z,8Z,11Z,13E-eicosatetraenoic acid (15-HETE) and arachidonic acid (peroxide free) were purchased from Cayman Chemical Company (Ann Arbor, MI). Spectrophotometric grade dimethyl sulfoxide (DMSO) was purchased from Sigma-Aldrich (Milwaukee WI), high purity methanol (MeOH), ethyl ether and acetic acid and other solvents were purchased from Fisher Scientific (Pittsburgh, PA). NADPH,

(±)-Metoprolol (+)-tartrate and (±)-verapamil hydrochloride was purchased from Sigma-Aldrich (St. Louis, MO). Warfarin was a kind gift from Dr. Thomas D. Nolin's lab. Human liver microsome (HLM) was purchased from CellzDirect (Carlsbad, CA). Rat liver microsomes (RLM) and recombinant CYP4F2 (rCYP4F2) were purchased from Seikisui Xenotech (Lenexa, KS). Rat kidney tissue was prepared by homogenization from male Sprague Dawley rats. RKM was prepared from differential centrifugation in a Beckman Coulter Optima XL-100K ultracentrifuge (Beckman Coulter, Fullerton, CA). Total protein concentration was determined by Lowry protein assay.

## **2.2 MICROSOMAL INCUBATION ASSAY**

### **2.2.1 AA Microsomal Incubation**

To screen the inhibitory effects against 20-HETE formation, compounds were tested in four different types of microsomes, including HLM, RLM, RKM or rCYP4F2. Compounds were dissolved in either 100% methanol or 100% DMSO to yield 10 mM stock solutions. Microsome incubation conditions were previously optimized. Microsomal incubations contained HLM, RLM, RKM (300 µg/ml) or rCYP4F2 (25 pmol/ml), AA (100 µM), NADPH (1 mM) and test compounds with various concentrations (50 nM to 2500 nM) in a 1 ml total volume in microsomal incubation buffer (0.12 M potassium phosphate buffer containing 5mM magnesium chloride). Each compound had three replications (n=3). Vehicle group was used as control to

calculate percentage of eicosanoids formation rate. HET0016 (250 nM) was used as positive control. Incubates without NADPH group served as the negative control.

Reaction was started by adding NADPH to the incubates and was carried out at 37 °C in a shaking water bath for 20 min. Reaction was stopped by placing tubes on ice, followed by adding 12.5 µl 20-HETE-d<sub>6</sub> as internal standard to each sample. Microsomal incubations were extracted with 3 ml ethyl ether twice, dried down under nitrogen gas and reconstituted in 125 µl 80:20 methanol: deionized H<sub>2</sub>O for analysis. 20-HETE formation was quantified using a validated UPLC-MS/MS assay and normalized by vehicle group [70]. Other eicosanoids including 15-, 12-HETEs, 8,9-, 11,12-, 14,15-EETs, and 5,6-, 8,9-, 11,12-, 14,15-DiHETs were monitored simultaneously.

### **2.2.2 Chromatographic Analysis of CYP Eicosanoids**

An Acquity ultra performance LC autosampler (Waters, Milford, MA) was used to separate HETEs, EETs and DiHETs on a UPLC BEH C18, 1.7 µm (2.1 × 100 mm) reversed-phase column (Waters, Milford, MA) protected by a guard column (2.1 × 5 mm; Waters, Milford, MA) of the same packing material. Column temperature was maintained at 55 °C. Mobile phases consisted of 0.005% acetic acid, 5% acetonitrile in deionized water (A) and 0.005% acetic acid in acetonitrile (B). The flow rate for mobile phases is 0.5 ml/min. The initial mixture of mobile phase was 65:35 of A and B. Mobile phase B increased at 0.4 minutes after injection from 35% to 70% in a linear gradient over 4 minutes, and again increased to 95% over 0.5 minutes where it remained for 0.3 minutes. This was followed by a linear return to initial conditions over 0.1

minutes with a 1.5 minute pre-equilibration period prior to the next sample run. Total run time was 6.4 minutes for each injection. Injection volumes were 7.5 $\mu$ l.

Mass spectrometric analysis was carried out using a TSQ Quantum Ultra (Thermo Fisher Scientific, San Jose, CA) triple quadrupole mass spectrometer using heated electrospray ionization (HESI). Mass spectrometer was operated in negative selective reaction monitoring (SRM) mode with unit resolutions at both Q1 and Q3 set at 0.70 Da full width at half maximum. Scan time was set at 0.01 s and collision gas pressure was 1.3 mTorr. Quantitation of HETEs, EETs, and DiHETs by SRM was performed by monitoring their m/z transitions. Analytical data was acquired and analyzed using Xcaliber 3.0 data system (ThermoFinnigan, San Jose, CA).

## **2.3 MICROSOMAL STABILITY ASSAY**

### **2.3.1 Compounds Microsomal Stability Assay**

Microsomal incubates contained HLM (500  $\mu$ g/ml), test compounds (1  $\mu$ M) and NADPH (1.3 mM) in a 1 ml total volume of microsomal incubation buffer (0.12 M potassium phosphate buffer containing 5mM magnesium chloride). Each compound had three replications (n=3).

Reaction was started by adding NADPH to the incubates and was carried out at 37  $^{\circ}$ C in a shaking water bath for 60 min. At 0, 15, 30, 45, 60 min, a 50  $\mu$ l aliquot of incubates was taken out and reaction was stopped by adding aliquot into 200  $\mu$ l ice-cold acetonitrile. After centrifugation at 14000 $\times$ g for 5 min, 200  $\mu$ l supernatant was taken out for UPLC-MS/MS analysis. Values at 0 min were used as corresponding control for test compounds. Varapamil,

metoprolol, and warfarin, categorized as fast, moderate and slow metabolism, were used as positive control. Incubates without NADPH group served as negative control.

### **2.3.2 Chromatographic Analysis Of Compounds**

Compounds were separated using the same instrument on a UPLC BEH C18, 1.7  $\mu\text{m}$  ( $2.1 \times 100$  mm) reversed-phase column (Waters, Milford, MA). Column temperature was maintained at 50  $^{\circ}\text{C}$ . Mobile phases consisted of 0.1% formic acid in deionized water (A) and acetonitrile (B) with a flow rate of 0.25 ml/min. The initial mixture of mobile phase was 80:20 of A and B. Mobile phase B increased from 20% to 95% at 0.5 minutes after injection in a linear gradient over 3 minutes and maintained for 0.5 minutes. This was followed by a linear return to initial conditions over 1.5 minutes. Total run time per sample was 5 minutes and all injection volumes were 7.5 $\mu\text{l}$ .

Mass spectrometric analysis was performed using a TSQ Quantum Ultra (Thermo Fisher Scientific, San Jose, CA) triple quadrupole mass spectrometer coupled with heated electrospray ionization (HESI) operated in positive selective reaction monitoring (SRM) mode with unit resolutions at both Q1 and Q3 set at 0.70 full width at half maximum. Quantitation by SRM analysis on compounds was performed by monitoring their m/z transitions. Scan time was set at 0.01 s and collision gas pressure was set at 1.2 mTorr. Analytical data was acquired and analyzed using Xcaliber 3.0 data system (ThermoFinnigan, San Jose, CA).



### **2.3 STATISTICAL ANALYSIS**

Data were analyzed with SPSS Statistics 23.0. Data were presented as mean  $\pm$  std of the percent of vehicle control. One-way ANOVA was carried out and corrected with Bonferroni as post-hoc test when comparing remaining 20-HETE between test compound group and vehicle group. Values that are statistically significant are designated by asterisks (\*,  $p < 0.05$ ).

## 3.0 RESULTS

### 3.1 COMPOUNDS 1-15 INHIBITORY EFFECT AGAINST 20-HETE FORMATION IN HLM, RLM, RKM AND rCYP4F2

Compounds **1-15** were obtained from a proprietary library that's available to our laboratory. HET0016 and 15 compounds were dissolved in methanol to yield 10 mM stock concentrations. Final concentrations of all the compounds in microsomal incubation buffer were 250 nM. HLM, RLM, RKM, and rCYP4F2 all produced 20-HETE only when incubated with AA in the presence of NADPH. HET0016, used as a positive control, completely knocked down 20-HETE formation in rCYP4F2, HLM, RLM and RKM by  $92.21 \pm 2.72\%$ ,  $98.3 \pm 0.37\%$ ,  $90.49 \pm 2.60\%$  and  $97.42 \pm 9.54\%$ , respectively. At 250 nM, compared with the no compound group, compound **3** and **10** significantly inhibited 20-HETE formation by  $51.60 \pm 3.32\%$  and  $53.62 \pm 5.93\%$  in rCYP4F2. Compounds **3**, **7**, **10** inhibited 20-HETE formation by  $21.00 \pm 6.60\%$ ,  $26.86 \pm 6.73\%$  and  $30.45 \pm 3.15\%$  in HLM, respectively, without statistical significance. Compounds **3**, **7**, **10** didn't show comparable inhibition effects in RLM or RKM as in rCYP4F2 or HLM. Interestingly, compound **14** and **15** only significantly decreased 20-HETE formation by  $32.55 \pm 0.83\%$  and

40.69±4.52% in RKM but not in HLM or RLM (**Figure 2**). **Table 2** lists inhibition of all 15 compounds against 20-HETE in percent of control in four different microsomes.

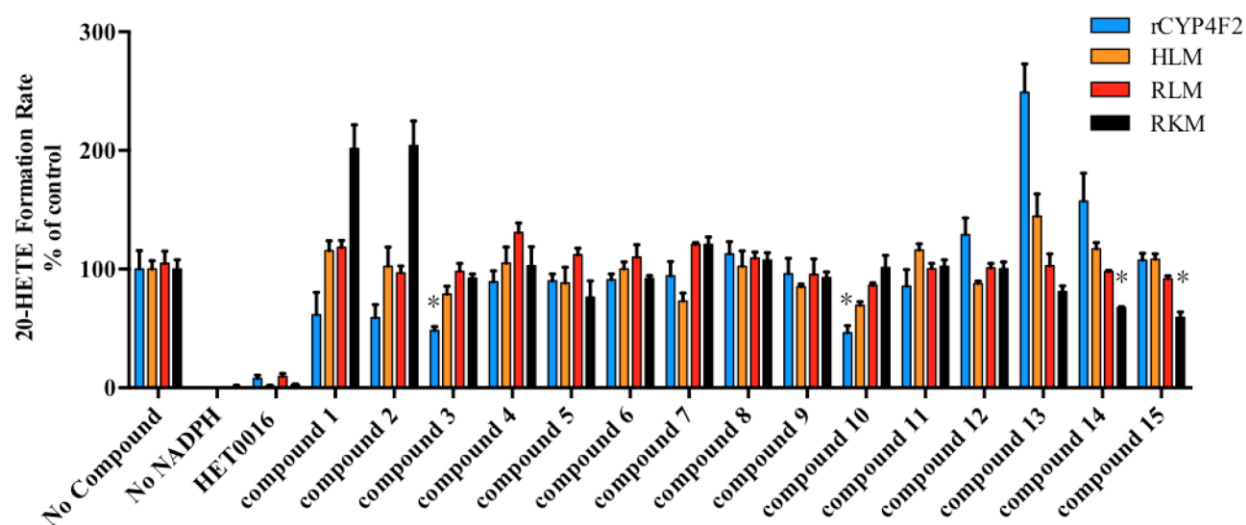


**Figure 2. Compounds 1-15 inhibition against 20-HETE formation in four different microsomes**

**Table 2. Compounds 1-15 inhibition against 20-HETE formation in percent of control**

Name	rCYP4F2	HLM	RLM	RKM
No compound	100±15.7%	100±7.08%	100±10.4%	100±7.96%
No NADPH	ND	0.03±0.04%	ND	0.73±1.46%
HET0016	7.79±2.72%	1.70±0.37%	9.51±2.60%	2.58±0.54%
Compound 1	61.6±18.8%	116±8.29%	118±5.77%	202±20.0%
Compound 2	59.1±10.9%	102±16.3%	96.9±5.71%	206±28.9%
Compound 3	48.4±3.32%*	79.0±6.60%	98.0±6.89%	92.4±3.55%
Compound 4	89.5±9.18%	105±13.4%	131±7.89%	110±16.1%
Compound 5	90.1±5.70%	88.3±13.4%	112±5.59%	76.5±13.7%
Compound 6	91.2±4.61%	100±5.98%	110±10.4%	92.2±2.35%
Compound 7	94.5±12.0%	73.1±6.73%	121±1.41%	121±6.09%
Compound 8	112±10.4%	102±13.1%	109±5.16%	108±6.14%
Compound 9	96.2±12.9%	85.1±2.24%	95.7±13.0%	92.8±4.89%
Compound 10	46.4±5.93%*	69.6±3.15%	86.5±1.92%	101±10.1%

Table 2 (continued)

Compound <b>11</b>	85.6±13.9%	116±5.24%	100±4.33%	102±5.49%
Compound <b>12</b>	129±13.9%	87.9±2.07%	101±3.8%	100±5.88%
Compound <b>13</b>	249±23.9%	145±18.9%	103±10.1%	81.1±4.80%
Compound <b>14</b>	157±23.5%	117±5.10%	97.8±1.06%	67.5±0.83%*
Compound <b>15</b>	108±5.77%	108±4.70%	91.9±2.37%	59.3±4.52%*

Based on the result in HLM, compounds **3**, **7**, and **10** were selected to conduct microsomal incubations in HLM with different concentrations. Methanol was used as vehicle control; it didn't inhibit 20-HETE formation at 1% (v/v). Compounds **3**, **7** and **10** all exhibited dose-dependent inhibition against 20-HETE formation in HLM (**Figure 3**). As concentration increased from 250 nM to 1000 nM to 2500 nM, compound **3** showed an increase in percent of inhibition from 7.17±9.28% to 20.32±6.53% to 31.09±2.14%. Compound **7** decreased 20-HETE formation by 35.99±2.90%, 59.43±1.25% and 75.40±0.42% at the three different concentrations. Compound **10** showed a similar trend with 31.59±3.00%, 62.68±1.45% and 76.05±5.45% at the three concentrations. After several repeat of the experiment, compound **10** consistently showed the best inhibition effect among all the compounds in HLM and good inhibition effect in rCYP4F2 and RLM. Based on these results, compound **10** could be a potential lead compound.

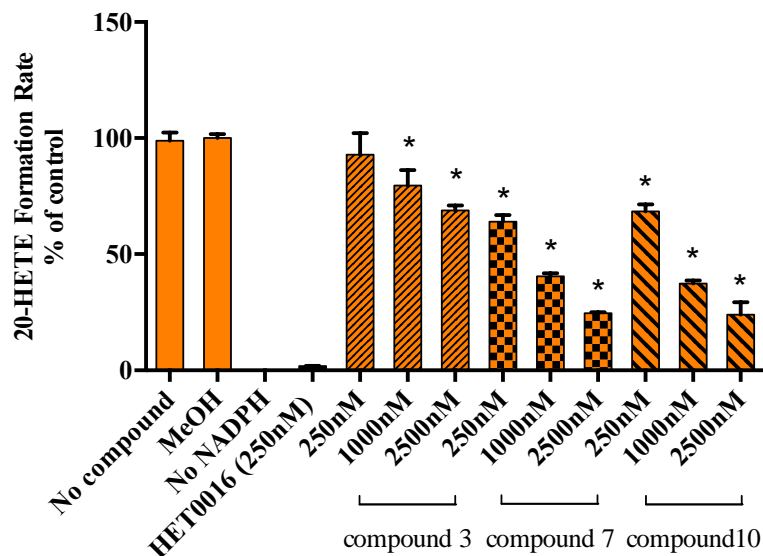


**Figure 3. Compounds 3, 7, and 10 dose-dependent inhibition against 20-HETE formation in HLM**

### **3.2 COMPOUNDS 21-26 INHIBITORY EFFECT AGAINST 20-HETE FORMATION IN HLM, RLM, RKM AND rCYP4F2**

Compounds **21** to **26** were selected from virtual screening and tested in four different types of microsomes for comparison with HET0016. Compounds were dissolved either in methanol or DMSO to yield a 10 mM stock solution. Final concentrations of test compounds and HET0016 were 2500 nM and 250 nM, respectively, in microsomal incubations. Methanol and DMSO were used as vehicle control for compounds dissolved in each solution. HLM, RLM, RKM and rCYP4F2 all produced 20-HETE in a NADPH-dependent manner. HET0016 inhibited 20-HETE formation profoundly in all four types of microsomes at 250 nM. At 2500 nM, compound **24** significantly reduced 20-HETE formation by  $12.82 \pm 2.26\%$  in RLM. Compound **25** significantly inhibited 20-HETE formation in both rCYP4F2 and HLM but not in RLM or RKM. It decreased

20-HETE by  $34.25 \pm 1.39\%$  and  $16.90 \pm 2.54\%$  in rCYP4F2 and HLM, respectively. Compound **26** reduced 20-HETE formation by  $65.16 \pm 5.13\%$ ,  $77.94 \pm 0.73\%$ ,  $12.94 \pm 4.71\%$  and  $24.84 \pm 4.26\%$  in rCYP4F2, HLM, RLM and RKM, respectively, with a lesser extent of inhibitory effect in RLM and RKM (Figure 4). Table 3 lists the remaining 20-HETE in percentage of control for six compounds in four types of microsomes.

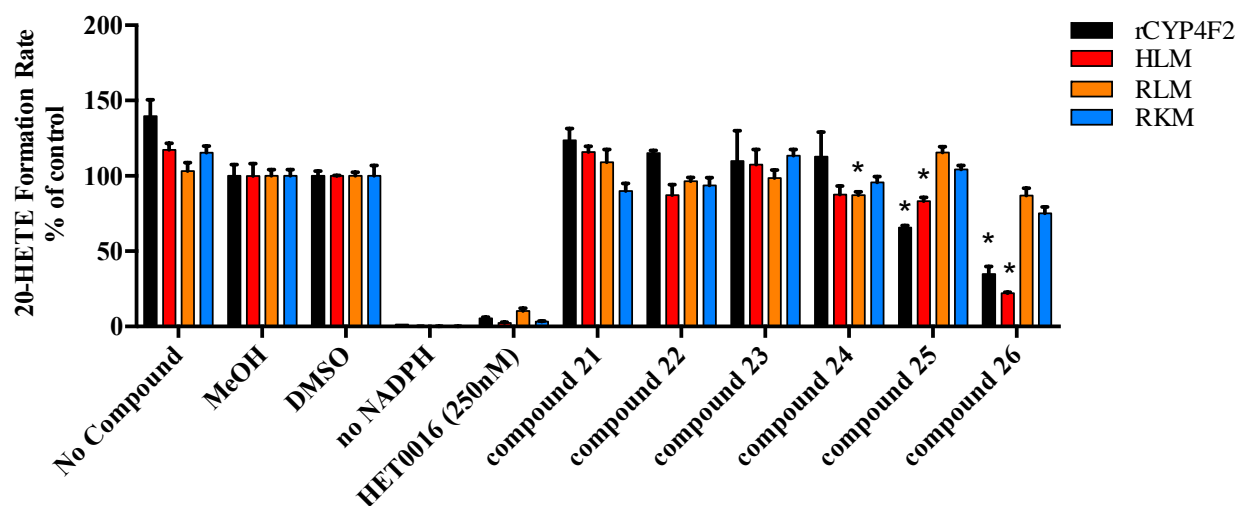


**Figure 4. Compounds 21-26 inhibitory effect against 20-HETE formation in four different microsomes**

**Table 3. Compounds 21-26 inhibition against 20-HETE formation in percent of control**

Name	rCYP4F2	HLM	RLM	RKM
No compound	140±10.8%	117±4.51%	103±5.46%	115±4.40%
MeOH	100±7.56%	100±8.08%	100±4.04%	100±4.19%
DMSO	100±3.23%	100±0.42%	100±2.41%	100±6.80%
No NADPH	1.47%	0.22±0.09%	0.19±0.10%	0.17±0.21%
HET0016	5.43±0.88%	2.39±0.52%	10.2±2.04%	3.34±0.42%
Compound <b>21</b>	124±7.79%	116±3.63%	109±8.50%	90.0±5.05%
Compound <b>22</b>	115±1.78%	108±10.0%	96.5±2.44%	93.9±5.03%

Compound <b>23</b>	110±20.3%	79.0±6.60%	98.7±5.24%	113±4.12%
Compound <b>24</b>	113±16.3%	87.5±5.80%	87.2±2.26%*	95.6±3.78%
Compound <b>25</b>	65.8±1.39%*	83.1±2.54%*	115±3.97%	104±2.53%
Compound <b>26</b>	34.8±5.14%*	22.1±0.73%*	87.1±4.71%	75.2±4.26%

Based on the previous 20-HETE inhibitory results in rCYP4F2 and HLM, compounds **25** and **26** were selected for further analysis in HLM at 250 nM, 1000 nM and 2500 nM. Compounds **25** and **26** both showed a dose-dependent inhibitory effect against 20-HETE formation. As concentration increased, remaining 20-HETE was 109.54±4.61%, 90.74±7.74% and 74.09±5.38% when treated with compound **25**. Compound **26** decreased 20-HETE formation by 45.21±10.81%, 62.57±4.67% and 73.87±0.83%, confirming that it could be a potential CYP4F2 enzyme inhibitor (**Figure 5**). Collectively, the initial screening in four different types of microsomes and dose-dependent inhibition results indicated that compound **10** and compound **26** could serve as lead compounds for optimization.

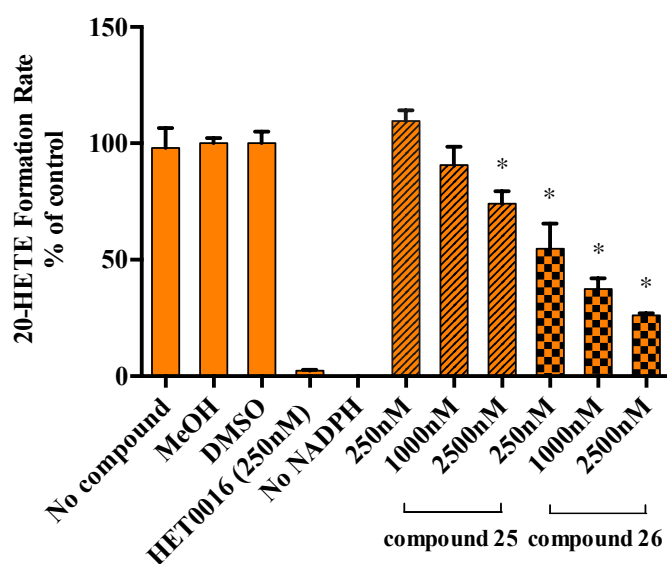


**Figure 5. Compounds 25 and 26 dose-dependent inhibition against 20-HETE formation in HLM**

**3.3 COMPOUNDS 16-19 INHIBITORY EFFECT AGAINST 20-HETE FORMATION IN HLM, RLM, RKM AND rCYP4F2**

Compounds **16**, **17**, **18**, and **19** were dissolved in DMSO to yield 10 mM stock concentrations. The final concentrations of all test compounds in the microsomal incubate was 2500 nM. HLM, RLM, RKM and rCYP4F2 all produced 20-HETE only in the presence of NADPH when incubated with AA. HET0016 completely blocked 20-HETE formation at 250 nM in rCYP4F2, HLM, RLM and RKM by  $95.62 \pm 0.90\%$ ,  $96.96 \pm 1.51\%$ ,  $86.39 \pm 0.21\%$  and  $97.33 \pm 0.04\%$ , respectively. At 2500 nM, compared with the corresponding vehicle group, compounds **18** and **19** significantly inhibited 20-HETE formation in all four microsomes. Compounds **18/19** inhibited 20-HETE formation by  $93.96 \pm 0.32\%/95.62 \pm 0.29\%$ ,  $90.18 \pm 1.56\%/91.40 \pm 1.34\%$ ,  $69.54 \pm 2.06\%/70.52 \pm 1.60\%$ , and  $46.95 \pm 1.02\%/27.82 \pm 1.72\%$  in rCYP4F2, HLM, RLM and RKM, respectively. Compound **17** significantly inhibited 20-HETE formation by  $82.43 \pm 2.53\%$ ,  $72.49 \pm 6.42\%$ ,  $41.95 \pm 0.83\%$  in rCYP4F2, HLM and RKM, except RLM (**Figure 6**). Table 4 lists percent of control of compounds **16-19** in four different microsomes.



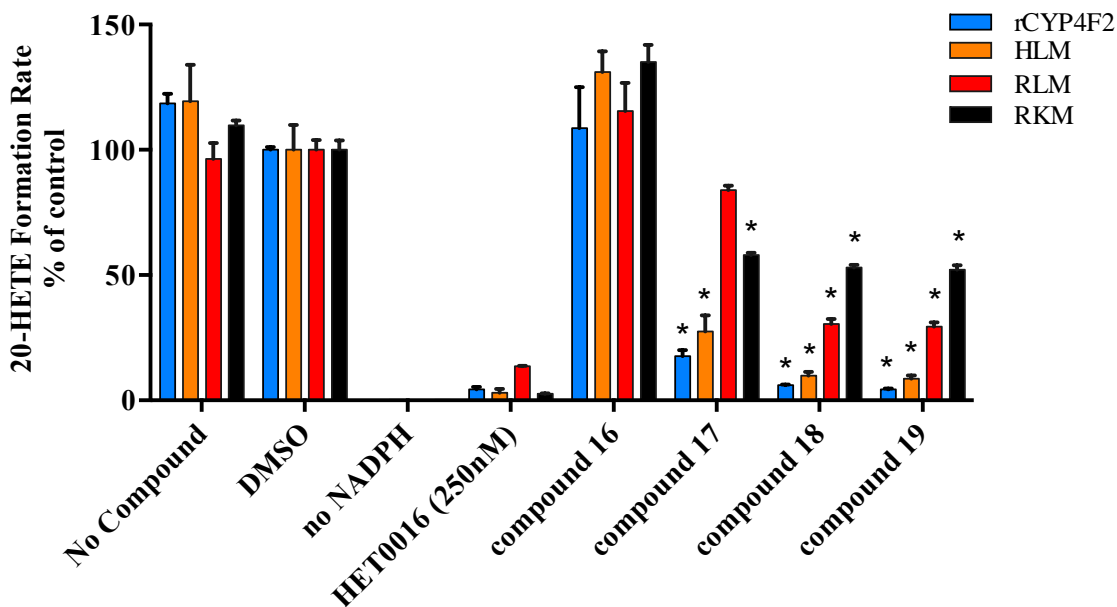


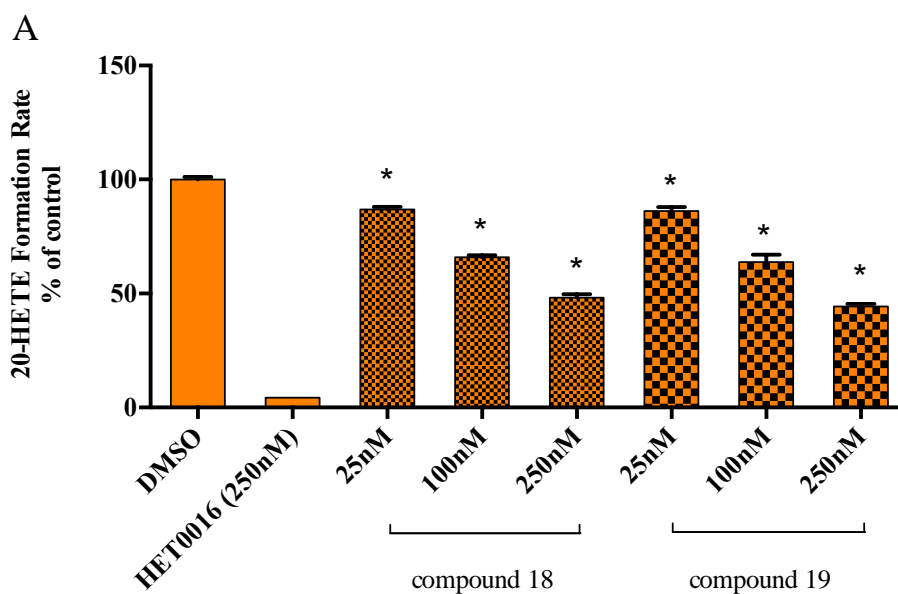
**Figure 6. Compounds 16-19 inhibitory effect against 20-HETE formation in four different microsomes**

**Table 4. Compounds 16-19 inhibition against 20-HETE formation in percent of control**

Name	rCYP4F2	HLM	RLM	RKM
No compound	119±3.80%	119±14.5%	96.3±6.46%	110±1.97%
DMSO	100±1.14%	100±9.94%	100±3.89%	100±3.76%
No NADPH	ND	0.21%	0.06%	0.24%
HET0016	4.38±0.90%	3.05±1.51%	13.6±0.21%	2.68±0.04%
Compound 16	109±16.4%	131±8.15%	115±11.3%	135±6.77%
Compound 17	17.6±2.53%*	27.5±6.42%*	83.9±1.86%	58.0±0.83%*
Compound 18	6.04±0.32%*	9.82±1.56%*	30.5±2.06%*	53.1±1.02%*
Compound 19	4.38±0.29%*	8.60±1.34%*	29.5±1.60%*	52.2±1.72%*

Compound **18** and **19** both dose-dependently inhibited 20-HETE formation in HLM (Figure 7A). As the concentration of these compounds increased from 25 nM to 100 nM to 250 nM, the inhibitory effect also increased. Compound **18** increased inhibition from 13.09 ± 1.12% to 34.12 ± 0.81% to 51.79 ± 1.45%, while compound **19** saw inhibition from 13.76 ± 1.64% to

36.24±3.24% to 55.68±1.21%, respectively. Based on these results, we could infer that the IC<sub>50</sub> value of compound **18/19** is less than 250 nM in HLM. Compound **18, 19** showed even better inhibitory effects against 20-HETE formation in rCYP4F2. Compound **18, 19** inhibited 20-HETE from 19.76±4.92% to 59.14±2.56% to 78.06±2.34% and 27.60±7.06% to 63.62±7.02% to 81.28±2.00%, respectively. IC<sub>50</sub> values of these compounds were less than 100 nM in rCYP4F2 (**Figure 7B**). As Figure 7 shows, compound **18** and **19** had improved inhibitory effect against 20-HETE formation compared with compound **10** or compound **26** at 250 nM.



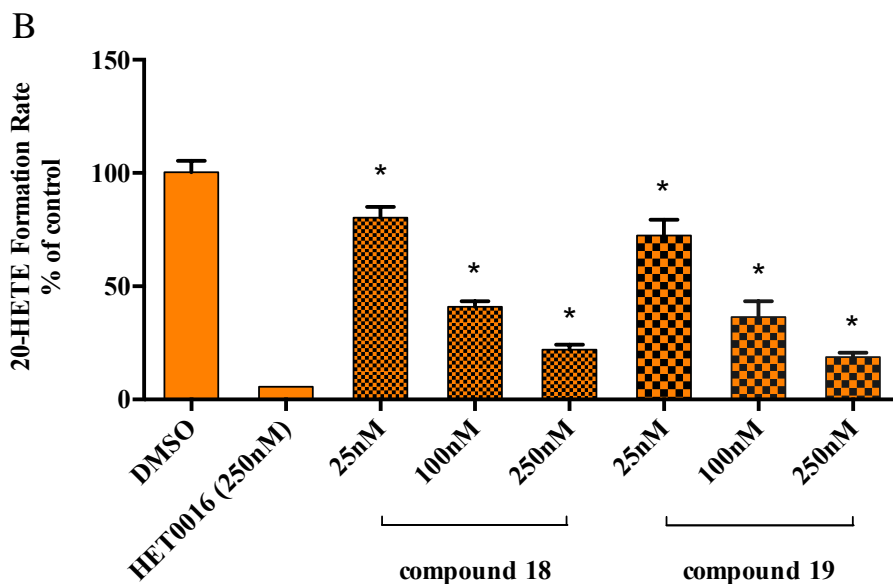


**Figure 7. Compounds 18 and 19 dose-dependent inhibition against 20-HETE formation in HLM (A) and rCYP4F2 (B).**

### 3.4 INHIBITORY EFFECT AGAINST EPOXYGENASE PATHWAY

As discussed in the introduction section, CYP450 epoxygenase pathway is responsible for EETs formation. EETs are vasodilators that have neuroprotective effect. Thus, 20-HETE as well as 8,9-, 11,12-, 14,15-EET and 5,6-, 8,9-, 11,12-, 14,15-DiHETs were monitored by UPLC-MS/MS simultaneously. Epoxygenase activity is reported by the sum of EETs and DiHETs as presented by percentage of control. In HLM, compound **10** (Figure 8A) inhibited 20-HETE formation in a dose-dependent manner, without inhibiting EETs or DiHETs formation. Compound **19** showed more potent inhibitory effect against 20-HETE formation, without inhibiting epoxygenase activity at 2500 nM (Figure 8B). Compound **26** (Figure 8C) showed 10-30% reduction in epoxygenase activity as concentration increased from 250 nM to 2500 nM. These data suggest

that compound **10** and compound **19** are potent 20-HETE formation inhibitors with IC<sub>50</sub> values in nanomolar range with good hydroxylase selectivity, where they didn't inhibit epoxygenase activity even at 2500 nM in HLM.

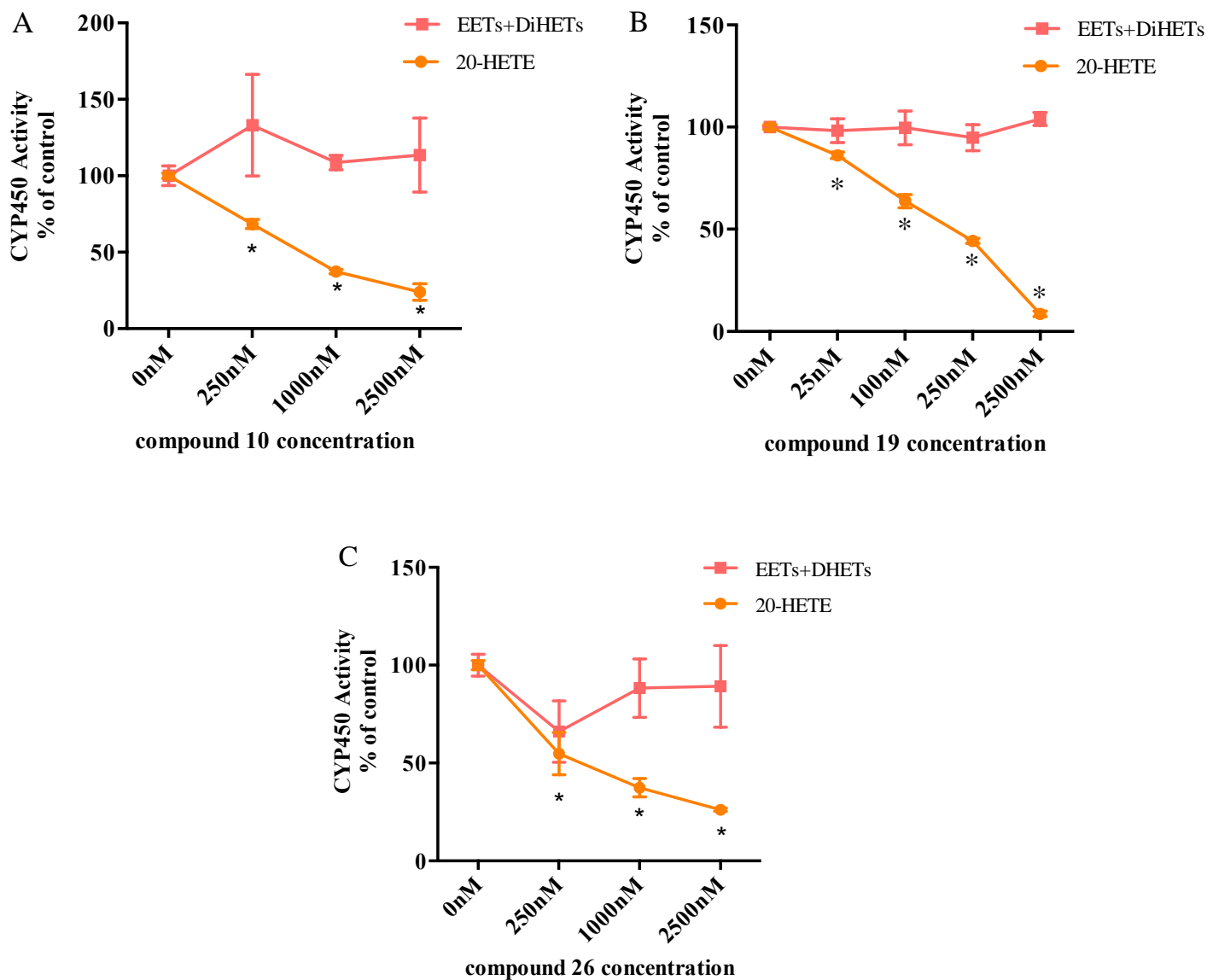


**Figure 8.** Compound **10** (A), compound **19** (B) and compound **26** (C) selectivity data in HLM.

### 3.5 MICROSOMAL STABILITY PROFILE OF COMPOUNDS

In early drug discovery process, compounds cannot be administered to human directly. In order to predict pharmacokinetic parameters like intrinsic clearance, *in vitro* systems are used. As compounds **10**, **19**, and **26** are promising as leads, we examined the metabolic stability of compounds **10**, **19**, and **26** in HLM. According to Nakamura et al., one pyrazole derivative of HET0016, 3-(4-n-Butoxyphenyl) pyrazole, had better solubility, stability under acidic environment and was also a selective potent 20-HETE inhibitor. 3-(4-n-butoxyphenyl)pyrazole was used as control since it already showed improved physicochemical properties compared with HET0016. Compounds **10**, **19**, **26** and 3-(4-n-butoxyphenyl)pyrazole were incubated in HLM during a 60-minute incubation time. 3-(4-n-butoxyphenyl)pyrazole had  $35.08 \pm 5.66\%$  remaining compound at the 30 min time point (Figure 9). Compared with 3-(4-n-butoxyphenyl)pyrazole, compound **26** was quickly metabolized with  $3.50 \pm 0.75\%$  remaining parent compound in incubates at 30 min. Compound **10** and compound **19** were slowly metabolized, with  $91.36 \pm 11.01\%$  and  $100.40 \pm 1.73\%$  remaining compound in HLM, respectively. These data suggest that our compounds **10** and **19** are more stable in *in vitro* human liver microsomal incubates and have better intrinsic clearance than their comparator and compound **26**.

Based on the results above, we will prioritize compound 10 as our lead compound to work with, as it has potent inhibition effect against 20-HETE and better stability compared with 3-(4-n-butoxyphenyl)pyrazole.

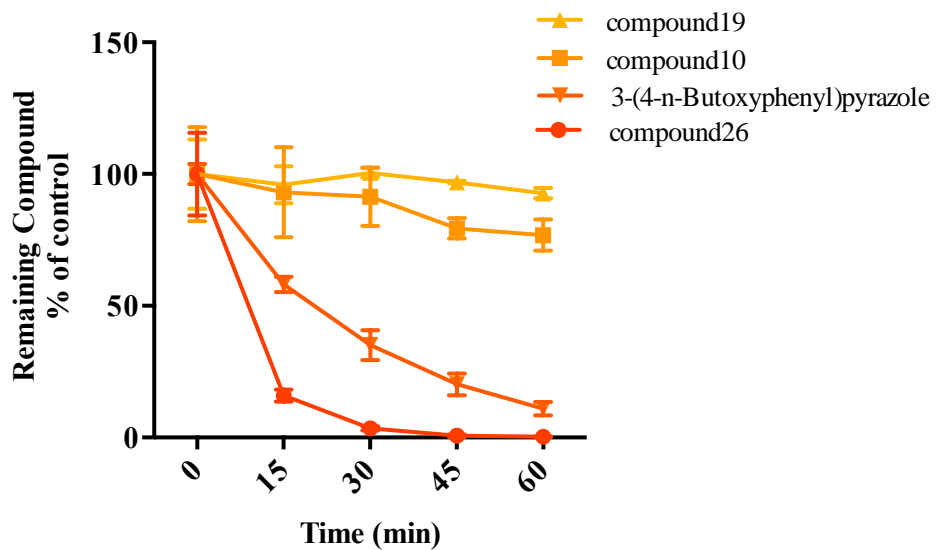


**Figure 9. Microsomal stability profile of compound 10, 19, 26 and 3-(4-n-Butoxyphenyl)pyrazole**

## 4.0 DISCUSSION

In this study, we identified three compounds 10, 19, and 26 as selective potent 20-HETE inhibitors that may serve as lead compounds for optimization by testing them in rCYP4F2, HLM, RLM, and RKM, together with stability assays..

### 4.1 INTERSPECIES DIFFERENCE

In order to examine the inhibition effect between different species and confirm inhibition specificity towards CYP4F2 isoform, rCYP4F2, HLM, RLM, and RKM were used as screening systems. Mean 20-HETE formation rate in HLM, RLM, RKM, rCYP4F2 without compound was 570.64, 629.81, 351.99 pmol/min/mg P450 and 0.52 pmol/min/pmol P450, respectively. 20-HETE was the most abundant metabolite in rCYP4F2, HLM, RLM and RKM. This is consistent with the finding that  $\omega$ -hydroxylation accounts for 50-75% of AA metabolism in humans, and 13-28% are EETs [149].

We observed interspecies difference in 20-HETE inhibition with test compounds. For example, compounds **10**, **18** and **19** inhibited 20-HETE in rCYP4F2 and HLM, but to a lesser extent in RLM and RKM. Compounds **14** and **15** only inhibited 20-HETE formation in RKM. Possible explanations include: (1) isoforms that are responsible for generating 20-HETE in humans and rats are different. CYP4A11 and 4F2 are major isoforms for 20-HETE formation in humans, while CYP4A1, 4A2 in rats. (2) Even if isoforms are same in different species, the difference in primary sequence of CYP protein will result in different substrate specificity. (3)

The level of CYP isoforms expression may be different in species. (4) There may be distinct catalytic activity for one substrate in different species as well [150]. For new drug development, isoform composition, expression and catalytic activity need to be considered when extrapolating preclinical data to humans.

#### **4.2 EFFECT OF ORGANIC SOLVENT ON METABOLIC ACTIVITY**

In the initial screening for compounds **1-15**, data were obtained by normalizing 20-HETE formation rate to no compound group. Compounds **3**, **7**, and **10** were selected and their inhibition data were then confirmed by normalizing formation rate by vehicle group in dose-dependent inhibition experiment. We observed that as methanol concentration increased from 0.25%, 0.5%, 0.75%, 1%, 2%, to 5%, there was a dose-dependent reduction in rCYP4F2 catalytic activity. Concentration at 1% for methanol or 0.5%: 0.5% methanol: DMSO did not significantly reduce 20-HETE formation. Methanol Concentration higher than 2% significantly reduced rCYP4F2 catalytic activity. The vehicle group (1% methanol or 0.5%: 0.5% methanol: DMSO) was used as control in subsequent analyses for all four types of microsomes. Chauret et al. evaluated methanol, DMSO, ACN on several HLM isoforms catalytic activity. Various isoforms were not affected by 1% methanol except for CYP2C8, 2C9, and 2E1 [151]. For CYP 2C8, 2C9, 2C19, 2E1, and 3A4 isoforms, even 0.2% DMSO inhibited their catalytic activity [151]. The presence of organic solvent may affect certain isoform catalytic activity. This should be taken into account when dissolving compound for inhibition study or examining compound *in vitro* metabolic pathways.



### 4.3 INDUCTION IN 20-HETE FORMATION

We observed compounds, such as compound **13**, showed an induction in 20-HETE formation. One possible explanation is enzyme activation. It had been reported that 7,8-benzoflavone as a CYP3A4 substrate itself, activated CYP3A4-catalyzed phenanthrene metabolism [152]. Shou et al. found that 7,8-benzoflavone didn't change  $K_m$  of phenanthrene metabolism, while increasing the  $V_{max}$  of phenanthrene metabolism and that phenanthrene didn't increase  $K_m$  of 7,8-benzoflavone metabolism, while decreasing the  $V_{max}$ , which indicated that more than one molecule could bind to CYP3A4 active sites simultaneously [152]. Subsequently, a two-substrate model was developed by the same laboratory, which could be used to explain phenanthrene/7,8-benzoflavone metabolism[153]. Phenanthrene and 7,8- benzoflavone serve as each other's effector of metabolism. 7,8-benzoflavone stimulates phenanthrene metabolism by 15.7-fold, while phenanthrene is a partial inhibitor of 7,8-benzoflavone metabolism. In the presence of the other substrate, binding constants are relatively unaffected. These data suggested that phenanthrene and 7,8-benzoflavone couldn't displace each other from the active site. In the presence of a certain compound, there is a possibility that AA still can bind to the active site of CYP4F2 or other isoforms that can convert AA, which may stimulate the generation 20-HETE. Compounds that showed an increase in 20-HETE formation need to undergo further experimental confirmation. Mechanisms of compounds inhibition towards CYP4F2 also need further elucidation.

#### **4.4 ENDOGENOUS OR EXOGENOUS COMPOUNDS THAT SHARE CYP4F2 METABOLISM PATHWAY**

To date, there have been several substrates of CYP4F2 being reported. CYP4F2 is responsible for  $\omega$ -hydroxylation of endogenous substrates AA and leukotriene B<sub>4</sub> (LTB<sub>4</sub>). CYP4A11 and 4F2 exhibited 20-HETE formation rate of 15.6 and 6.8 nmol/min/nmol P450, while antibodies to CYP4F2 inhibited 20-HETE formation by 93.4% [47]. Leutotriene B<sub>4</sub> is a derivative of AA, which can be converted to 20-hydroxyleukotriene B<sub>4</sub> by CYP4F2 at a turnover rate of 392 pmol/min/nmol P450 [154]. CYP4F2 is also an oxidase for vitamin K, which is associated with warfarin dosage. McDanold et al. showed that CYP4F2 V433M (rs2108622) allele have a reduced capacity to metabolize vitamin K<sub>1</sub> in human liver microsomes [155]. This could be an explanation for high inter-individual variability in warfarin dosage. A meta-analysis that includes 13 clinical studies showed that patients with CYP4F2 CT and TT genotypes require 10% and 21% higher warfarin doses [156].

CYP4F2 also plays a role in metabolizing xenobiotics. Fingolimod is a FDA approved treatment for relapsing multiple sclerosis. Jin et al. reported that only recombinant human CYP4F2 and to some extent CYP4F3B produced fingolimod metabolites similar to those in HLM, and an antibody of CYP4F2 inhibited fingolimod metabolism completely in HLM [157]. Brincidofovir (CMX001) is an antiviral drug for treating cytomegalovirus, adenovirus, smallpox, and ebolavirus infections currently in Phase III clinical trials. Tippin et al. demonstrated that CYP4F2 is the major enzyme involved in CMX001 metabolism by the data that CMX001 metabolism was inhibited by HET0016 and ketoconazole in both HLM and human rCYP4F2.

CYP4F2 is also responsible for  $\omega$ -hydroxylation for tocopherol and tocotrienol. This is supported by the results that human rCYP4F2 oxidized tocopherol into its terminal hydroxylated and carboxylated metabolites, and 1  $\mu$ M sesamin inhibited tocopherol metabolism in rCYP4F2, HLM, and RLM by more than 80% [158]. Vitamin E is composed of tocopherols and tocotrienols. Thus, CYP4F2 plays a role in regulating vitamin E metabolism. In insect cells that express wild type or polymorphic variants of the human CYP4F2, the W12G variant had two-fold higher enzymatic activity towards tocopherols and tocotrienols, whereas the V433 variant showed one half of the enzymatic activity compared with wild type [159].

The expression level of CYP4F2 may have effects when considering results in humans. Lasker's group developed an antibody to quantify CYP4F2 expression in human liver and kidney, which is able to differentiate between CYP4F2, 4F3B, 4F11 and 4F12 [147]. They found CYP4F2 expression is highly variable (0-80.1 pmol/mg microsomal protein) in human liver microsome from 29 subjects pool with a mean of  $18.2 \pm 19.9$  pmol/mg [147]. CYP4F2 has lower level and less variability in human kidney microsomes (n=10), ranging from 0 – 11.3 pmol/mg microsomal protein with a mean of  $3.9 \pm 3.8$  pmol/mg [147]. Subsequently, the pie chart of human liver CYP450 pie chart was updated for CYP4F subfamily, CYP4F enzymes account for approximately 15% of total CYP450 enzymes in human liver [160].

Thus, enzymatic inhibition of CYP4F2 may induce changes in endogenous or exogenous substrates metabolism. 20-HETE metabolism pathway needs to be further elucidated, as well as CYP4F2 polymorphism need to be considered to better predict potential interactions between substrates being metabolized by CYP4F2.

## 4.5 PHYSICOCHEMICAL PROPERTIES FOR DRUGGABLE COMPOUNDS

In order to optimize compounds to increase potency and selectivity, Lipinski rule of fives (RO5) is used to evaluate druglikeness properties. RO5 include: (1) molecular weight  $\leq 500$ , (2) LogP (the logarithm of the partition coefficient between water and 1-octanol)  $\leq 5$ , (3) H-bond donors  $\leq 5$ , (4) H-bond acceptors  $\leq 10$  [161]. When aiming to produce neuroprotective effects in the brain, compounds with molecular weight  $\leq 450$ , LogP values ranging between 1.5-2.7, heteroatoms capable of hydrogen bonding (O+N)  $\leq 5$ , PSA within 60-70Å, rotatable bonds  $\leq 5$ , and pKa around 7-8 showed good BBB penetration [162].

Physicochemical characteristics of compounds need to be considered during optimization of lead compound identified in our study. When advancing from preclinical to clinical studies, physicochemical properties, pharmacokinetic parameters including metabolic stability, metabolic liability, permeability and protein binding as well as patients pathophysiological need to be accounted to select the most appropriate drug candidate.

## 4.6 sEH INHIBITION OR 20-HETE INHIBITION

20-HETE and sEH have been investigated as potential therapeutic targets for cerebral vascular diseases. Both 20-HETE inhibition and sEH inhibition or sEH gene deletion demonstrated positive neurological outcome. The major holdback for investigating 20-HETE pathogenesis role in human is lacking suitable druggable inhibitor. In 2005, TS-011 was in a phase I clinical trial in acute ischemic stroke patients. However, with no follow-up information provided, it is likely that

TS-011 failed in phase I clinical trial for some unknown reason. Sesamin is the other 20-HETE inhibitor that underwent clinical trials. Overweight men and postmenopausal women receiving sesame bar (providing 26.2 g of sesame seeds per day) had 28% reduction in plasma unesterified 20-HETE levels and a 32% reduction in urinary excretion [115]. On the contrary, sEH inhibitors progressed further in clinical trials. AR9281, a sEH inhibitor, was in phase IIa clinical trials in pre-diabetic patients, but failed to show efficacy in early-stage hypertension. EC5026 is a novel sEH inhibitor that showed efficacy in diabetic neuropathic pain, and phase I clinical trial will be initiated to study safety profile of EC5026.

20-HETE synthase inhibitors and 20-HETE receptor antagonists have their pros and cons. 20-HETE synthase inhibitors works on the enzymes that form 20-HETE, such as CYP4A or CYP4F subfamilies. However, inhibiting the enzymes may lead to disruptions of metabolism of other endogenous or exogenous compounds, like vitamin K. To date, there have been no explicit 20-HETE receptors being reported, antagonists were designed based on the structure of 20-HETE. 20-HETE antagonists compete with 20-HETE to bind with the receptor, thus leaves the substrates that metabolized by the enzymes unaffected. However, receptor antagonists inhibit effects of preformed 20-HETE if present in esterified lipids in the membrane, and we are not clear right now that if there are other ligands that work through that receptor or not. Further considerations and studies will be needed to elucidate the difference between this two strategies.

sEH is a promising therapeutic target in cardiovascular diseases. Inhibiting sEH to increase EETs showed favorable outcomes in spontaneously hypertensive stroke-prone rats [163]. However, sEH gene deletion may result a shift in HETEs production. For example, while kidney homogenates from sEH gene deletion mice had lower DiHETs levels and higher EETs levels, 20-HETE levels increased by four fold [164]. Plasma concentration of 9-, 11-, 15-, 19-HETE

was increased by two fold in sEH gene knockout mice [165]. This suggests that hydroxylase activity is increased in sEH gene knockout mice.

Inhibition of 20-HETE provided beneficial effects in cardiovascular and cerebrovascular diseases. Reduction in 20-HETE formation improves CBF and neurological outcomes. Enzymes that metabolize AA also metabolize exogenous compounds. Inhibiting enzymes that are responsible for 20-HETE formation may lead to alterations of enzyme substrate levels. The role of 20-HETE is the basis that produces deleterious effects in diseases. Targeting 20-HETE formation is aiming at the origin that causes neurological deficits. In acute ischemic stroke patients, baseline 20-HETE level was positively associated with lesion size, but not EETs or DiHETs [89]. 20-HETE was also associated with functional indices including greater neurological impairment, reduced modified barthel index (MBI), and reduced cognitive function, while EETs or DiHETs had no association with functional indices. Further studies need to be carried out to compare the beneficial effects of two strategies, or testing if sEH inhibition plus 20-HETE inhibition will have synergistic effects in cerebral vascular and cardiovascular diseases.

## 5.0 CONCLUSION

To summarize, in the work we screened 26 compounds, compounds **10**, **19**, and **26** were potent 20-HETE formation inhibitors with an  $IC_{50}$  value in nano molar range. Compounds **10** and **19** dose-dependently inhibited 20-HETE formation and showed good selectivity for hydroxylase pathway, they didn't inhibit epoxygenase at 2500 nM. Compound **26** decreased epoxygenase activity for around 10-30%. Compounds **10** and **19** were metabolically stable in HLM though out a 60-minute incubation period, while compound **26** was quickly metabolized within 30 minutes. Thus, compound **10**, **19**, and **26** can serve as lead compounds for structure optimization, and we will prioritize with compound **10** and **19**.

## 6.0 FUTURE DIRECTION

Experiments need to be conducted to obtain  $IC_{50}$  values of lead compounds in order to confirm compounds inhibition potency. More selectivity evaluation of compound inhibition against other CYP isoforms will need to be done to provide evidence if compounds are selective to isoforms that only produce 20-HETE instead of other drug metabolizing CYP enzymes. More compounds will need to be experimentally tested *in vitro* in order to select a potential *in vivo* candidate. Also, lead compounds incubated in brain microsomes would give relevant information towards eicosanoids enzymatic formation in the brain. The ultimate goal at the current state is to screen and identify the compound that has the optimum physicochemical properties, including potency, solubility, selectivity, microsomal stability and ability to across BBB. CYP4F2 homology model will be optimized based on the screening results at the same time to support compound design and virtual screening.



## APPENDIX. ABBREVIATION

4-PCO	4-phenylchalcone oxide
10-SUYS	10-undecynyl sulfate
17-ODYA	17-octadecynoic acid
20-HETE	20-hydroxyeicosatetraenoic acid
20-SOLA	2,5,8,11,14,17-hexaoxonadecan-19-yl-20-hydroxyeicosa-6(Z),15(Z)-dienoate
AA	Arachidonic acid
ABT	1-aminobenzotriazole
AHA	American Heart Association
ASA	American Stroke Association
aSAH	Aneurysmal subarachnoid hemorrhage
BBB	Blood brain barrier
CA	Cardiac arrest
CBF	Cerebral blood flow
CO	Carbon monoxide
COX	Cyclooxygenase
cPLA <sub>2</sub>	Cytosolic phospholipase A2
CPP	Cerebral perfusion pressure
CPR	Cardiopulmonary resuscitation
CSF	Cerebral spinal fluid
CPP	Cerebral perfusion pressure
CYP	Cytochrome P450
DBDD	12,12-dibromododec-11-enoic acid
DCI	Delayed cerebral ischemia
DDMS	N-methylsulfonyl-12,12-dibromododec-11-enamide
DiHET	Dihydroxyeicosatrienoic acid
DPMS	N-methylsulfonyl-15,15-dibromopentadec-14-enamide
EET	Epoxyeicosatrienoic acid
EBI	Early brain injury
eNOS	Endothelial nitric oxide synthase

FDA	Food and Drug Administration
HET0016	N-hydroxy-N-(4-butyl-2-methylphenyl) formamidine
ICP	Intracranial pressure
ICH	Intracerebral hemorrhage
LOX	Lipoxygenase
LTB4	Leukotriene B4
MCAO	Middle cerebral artery occlusion
MS/MS	Tandem mass spectrometry
NADPH	Nicotinamide adenine dinucleotide phosphate
NO	Nitric oxide
PGF <sub>2α</sub>	Prostaglandin F <sub>2α</sub>
PGI <sub>2</sub>	Prostacyclin
PPAR	Peroxisome proliferator-activated receptor alpha
PSA	Polar surface area
rt-PA	Recombinant tissue-type plasminogen activator
SAH	Subarachnoid hemorrhage
sEH	Soluble epoxide hydrolase
SKF-525A	β-diethyl-aminoethyldiphenylpropylacetate
SRM	Selective reaction monitoring
TIA	Transient ischemic attack
TS-011	N-(3-chloro-4-morpholin-4-yl) phenyl-N'-hydroxyimido formamide
TXA <sub>2</sub>	Thromboxane A2
TXB <sub>2</sub>	Thromboxane B2
UPLC	Ultra-performance liquid chromatography

## BIBLIOGRAPHY

1. Mozaffarian, D., et al., *Heart Disease and Stroke Statistics—2016 Update: A Report From the American Heart Association*. Circulation, 2015.
2. Deb, P., S. Sharma, and K.M. Hassan, *Pathophysiologic mechanisms of acute ischemic stroke: An overview with emphasis on therapeutic significance beyond thrombolysis*. Pathophysiology, 2010. **17**(3): p. 197-218.
3. Durukan, A. and T. Tatlisumak, *Acute ischemic stroke: Overview of major experimental rodent models, pathophysiology, and therapy of focal cerebral ischemia*. Pharmacology Biochemistry and Behavior, 2007. **87**(1): p. 179-197.
4. Ergul, A., A. Alhusban, and S.C. Fagan, *Angiogenesis: A Harmonized Target for Recovery After Stroke*. Stroke, 2012. **43**(8): p. 2270-2274.
5. Pan, J., et al., *Reperfusion injury following cerebral ischemia: pathophysiology, MR imaging, and potential therapies*. Neuroradiology, 2007. **49**(2): p. 93-102.
6. Khatri, R., et al., *Blood–brain barrier, reperfusion injury, and hemorrhagic transformation in acute ischemic stroke*. Neurology, 2012. **79**(13 Supplement 1): p. S52-S57.
7. Hillis, A.E., et al., *Perfusion-weighted MRI as a marker of response to treatment in acute and subacute stroke*. Neuroradiology, 2004. **46**(1): p. 31-39.
8. Adams, H.P., et al., *Guidelines for the Early Management of Adults With Ischemic Stroke: A Guideline From the American Heart Association/American Stroke Association Stroke Council, Clinical Cardiology Council, Cardiovascular Radiology and Intervention Council, and the Atherosclerotic Peripheral Vascular Disease and Quality of Care Outcomes in Research Interdisciplinary Working Groups: The American Academy of Neurology affirms the value of this guideline as an educational tool for neurologists*. Circulation, 2007. **115**(20): p. e478-e534.
9. The, N.t.-P.A.S.S.G., *Intracerebral Hemorrhage After Intravenous t-PA Therapy for Ischemic Stroke*. Stroke, 1997. **28**(11): p. 2109-2118.
10. Kernan, W.N., et al., *Guidelines for the Prevention of Stroke in Patients With Stroke and Transient Ischemic Attack: A Guideline for Healthcare Professionals From the American Heart Association/American Stroke Association*. Stroke, 2014. **45**(7): p. 2160-2236.
11. Durrant, J.C. and H.E. Hinson, *Rescue Therapy for Refractory Vasospasm after Subarachnoid Hemorrhage*. Current neurology and neuroscience reports, 2015. **15**(2): p. 521-521.
12. Nieuwkamp, D.J., et al., *Changes in case fatality of aneurysmal subarachnoid haemorrhage over time, according to age, sex, and region: a meta-analysis*. The Lancet Neurology, 2009. **8**(7): p. 635-642.
13. Rodr, R., et al., *Predictor's of Mortality in Patients with Aneurysmal Subarachnoid Haemorrhage and Rebleeding*. Vol. 2015. 2015. 6.
14. Kusaka, G., et al., *Signaling Pathways for Early Brain Injury after Subarachnoid Hemorrhage*. Journal of Cerebral Blood Flow & Metabolism, 2004. **24**(8): p. 916-925.
15. Cahill, W.J., J.H. Calvert, and J.H. Zhang, *Mechanisms of Early Brain Injury after Subarachnoid Hemorrhage*. Journal of Cerebral Blood Flow & Metabolism, 2006. **26**(11): p.

- 1341-1353.
16. Sabri, M., E. Lass, and R.L. Macdonald, *Early Brain Injury: A Common Mechanism in Subarachnoid Hemorrhage and Global Cerebral Ischemia*. Vol. 2013. 2013. 9.
  17. Schubert, G.A., et al., *Hypoperfusion in the Acute Phase of Subarachnoid Hemorrhage*. 2011: p. 35-38.
  18. Carr, K.R., S.L. Zuckerman, and J. Mocco, *Inflammation, Cerebral Vasospasm, and Evolving Theories of Delayed Cerebral Ischemia*. Vol. 2013. 2013. 12.
  19. Dhar, R., et al., *Relationship between Angiographic Vasospasm and Regional Hypoperfusion In Aneurysmal Subarachnoid Hemorrhage*. *Stroke; a Journal of Cerebral Circulation*, 2012. **43**(7): p. 1788-1794.
  20. Vergouwen, M.D.I., et al., *Definition of Delayed Cerebral Ischemia After Aneurysmal Subarachnoid Hemorrhage as an Outcome Event in Clinical Trials and Observational Studies: Proposal of a Multidisciplinary Research Group*. *Stroke*, 2010. **41**(10): p. 2391-2395.
  21. Macdonald, R.L., et al., *Clazosentan to Overcome Neurological Ischemia and Infarction Occurring After Subarachnoid Hemorrhage (CONSCIOUS-1): Randomized, Double-Blind, Placebo-Controlled Phase 2 Dose-Finding Trial*. *Stroke*, 2008. **39**(11): p. 3015-3021.
  22. Dhar, R. and M.N. Diringer, *Relationship Between Angiographic Vasospasm, Cerebral Blood Flow, and Cerebral Infarction After Subarachnoid Hemorrhage*. 2015: p. 161-165.
  23. Adamczyk, P., et al., *Medical Management of Cerebral Vasospasm following Aneurysmal Subarachnoid Hemorrhage: A Review of Current and Emerging Therapeutic Interventions*. Vol. 2013. 2013. 10.
  24. Mozaffarian, D., et al., *Heart Disease and Stroke Statistics—2015 Update: A Report From the American Heart Association*. *Circulation*, 2015. **131**(4): p. e29-e322.
  25. Nolan, J.P., et al., *Post-cardiac arrest syndrome: Epidemiology, pathophysiology, treatment, and prognostication: A Scientific Statement from the International Liaison Committee on Resuscitation; the American Heart Association Emergency Cardiovascular Care Committee; the Council on Cardiovascular Surgery and Anesthesia; the Council on Cardiopulmonary, Perioperative, and Critical Care; the Council on Clinical Cardiology; the Council on Stroke*. *Resuscitation*, 2008. **79**(3): p. 350-379.
  26. Manole, M.D., et al., *Post-Cardiac Arrest Syndrome: Focus on the Brain*. *Current opinion in pediatrics*, 2009. **21**(6): p. 745-750.
  27. Rolfsen, M.L. and W.R. Davis, *Cerebral function and preservation during cardiac arrest*. *Critical Care Medicine*, 1989. **17**(3).
  28. Buunk, G., J.G. van der Hoeven, and A.E. Meinders, *Cerebral blood flow after cardiac arrest*. *The Netherlands Journal of Medicine*, 2000. **57**(3): p. 106-112.
  29. Koehler, R.C., et al., *Augmentation of cerebral perfusion by simultaneous chest compression and lung inflation with abdominal binding after cardiac arrest in dogs*. *Circulation*, 1983. **67**(2): p. 266-275.
  30. Holzer, M., et al., *Endothelin-1 elevates regional cerebral perfusion during prolonged ventricular fibrillation cardiac arrest in pigs*. *Resuscitation*, 2002. **55**(3): p. 317-327.
  31. Krep, H., et al., *Treatment with an endothelin type A receptor-antagonist after cardiac arrest and resuscitation improves cerebral hemodynamic and functional recovery in rats*. *Critical Care Medicine*, 2000. **28**(8).
  32. KUBOYAMA, K., et al., *Delay in cooling negates the beneficial effect of mild resuscitative cerebral hypothermia after cardiac arrest in dogs: A prospective, randomized study*. *Critical*

- Care Medicine, 1993. **21**(9): p. 1348-1358.
33. STERZ, F., et al., *Mild hypothermia cardiopulmonary resuscitation improves outcome after prolonged cardiac arrest in dogs*. Critical Care Medicine, 1991. **19**(3): p. 379-389.
  34. Hicks, S.D., D.B. DeFranco, and C.W. Callaway, *Hypothermia during Reperfusion after Asphyxial Cardiac Arrest Improves Functional Recovery and Selectively Alters Stress-Induced Protein Expression*. Journal of Cerebral Blood Flow & Metabolism, 2000. **20**(3): p. 520-530.
  35. Hickey, R.W., et al., *Delayed, spontaneous hypothermia reduces neuronal damage after asphyxial cardiac arrest in rats*. Critical Care Medicine, 2000. **28**(10).
  36. Bernard, S.A., et al., *Treatment of Comatose Survivors of Out-of-Hospital Cardiac Arrest with Induced Hypothermia*. New England Journal of Medicine, 2002. **346**(8): p. 557-563.
  37. Nunnally, M.E., et al., *Targeted temperature management in critical care: A report and recommendations from five professional societies\**. Critical Care Medicine, 2011. **39**(5).
  38. Vaity, C., N. Al-Subaie, and M. Cecconi, *Cooling techniques for targeted temperature management post-cardiac arrest*. Critical Care, 2015. **19**(1): p. 103.
  39. Zeldin, D.C., *Epoxygenase pathways of arachidonic acid metabolism*. J Biol Chem, 2001. **276**(39): p. 36059-62.
  40. Roman, R.J., *P-450 metabolites of arachidonic acid in the control of cardiovascular function*. Physiol Rev, 2002. **82**(1): p. 131-85.
  41. Holtzman, M.J., *Arachidonic Acid Metabolism: Implications of Biological Chemistry for Lung Function and Disease*. American Review of Respiratory Disease, 1991. **143**(1): p. 188-203.
  42. Capdevila, J.H., J.R. Falck, and R.C. Harris, *Cytochrome P450 and arachidonic acid bioactivation: molecular and functional properties of the arachidonate monooxygenase*. Journal of Lipid Research, 2000. **41**(2): p. 163-181.
  43. Oliw, E.H., *bis-Allylic hydroxylation of linoleic acid and arachidonic acid by human hepatic monooxygenases*. Biochimica et Biophysica Acta (BBA) - Lipids and Lipid Metabolism, 1993. **1166**(2): p. 258-263.
  44. El-Sherbeni, A.A. and A.O.S. El-Kadi, *Repurposing Resveratrol and Fluconazole To Modulate Human Cytochrome P450-Mediated Arachidonic Acid Metabolism*. Molecular Pharmaceutics, 2016. **13**(4): p. 1278-1288.
  45. Harder, D.R., et al., *Formation and action of a P-450 4A metabolite of arachidonic acid in cat cerebral microvessels*. American Journal of Physiology - Heart and Circulatory Physiology, 1994. **266**(5): p. H2098-H2107.
  46. Arnold, C., et al., *Arachidonic Acid-metabolizing Cytochrome P450 Enzymes Are Targets of  $\omega$ -3 Fatty Acids*. Journal of Biological Chemistry, 2010. **285**(43): p. 32720-32733.
  47. Powell, P.K., et al., *Metabolism of Arachidonic Acid to 20-Hydroxy-5,8,11,14-eicosatetraenoic Acid by P450 Enzymes in Human Liver: Involvement of CYP4F2 and CYP4A11*. Journal of Pharmacology and Experimental Therapeutics, 1998. **285**(3): p. 1327-1336.
  48. Lasker, J.M., et al., *Formation of 20-Hydroxyeicosatetraenoic Acid, a Vasoactive and Natriuretic Eicosanoid, in Human Kidney: ROLE OF CYP4F2 AND CYP4A11*. Journal of Biological Chemistry, 2000. **275**(6): p. 4118-4126.
  49. Fer, M., et al., *Cytochromes P450 from family 4 are the main omega hydroxylating enzymes in humans: CYP4F3B is the prominent player in PUFA metabolism*. Journal of Lipid Research, 2008. **49**(11): p. 2379-2389.

50. Kalsotra, A., et al., *Renal localization, expression, and developmental regulation of P450 4F cytochromes in three substrains of spontaneously hypertensive rats*. *Biochemical and Biophysical Research Communications*, 2005. **338**(1): p. 423-431.
51. Chuang, S.S., et al., *CYP2U1, a Novel Human Thymus- and Brain-specific Cytochrome P450, Catalyzes  $\omega$ - and ( $\omega$ -1)-Hydroxylation of Fatty Acids*. *Journal of Biological Chemistry*, 2004. **279**(8): p. 6305-6314.
52. Nguyen, X., et al., *Kinetic profile of the rat CYP4A isoforms: arachidonic acid metabolism and isoform-specific inhibitors*. *American Journal of Physiology - Regulatory, Integrative and Comparative Physiology*, 1999. **276**(6): p. R1691-R1700.
53. Xu, F., et al., *Catalytic Activity and Isoform-Specific Inhibition of Rat Cytochrome P450 4F Enzymes*. *Journal of Pharmacology and Experimental Therapeutics*, 2004. **308**(3): p. 887-895.
54. Ito, O., et al., *Localization of cytochrome P-450 4A isoforms along the rat nephron*. *American Journal of Physiology - Renal Physiology*, 1998. **274**(2): p. F395-F404.
55. Hoch, U., et al., *Structural Determination of the Substrate Specificities and Regioselectivities of the Rat and Human Fatty Acid  $\omega$ -Hydroxylases*. *Archives of Biochemistry and Biophysics*, 2000. **373**(1): p. 63-71.
56. Kalsotra, A., et al., *Sexual Dimorphism and Tissue Specificity in the Expression of CYP4F Forms in Sprague Dawley Rats*. *Drug Metabolism and Disposition*, 2002. **30**(9): p. 1022-1028.
57. Kroetz, D.L. and F. Xu, *REGULATION AND INHIBITION OF ARACHIDONIC ACID  $\omega$ -HYDROXYLASES AND 20-HETE FORMATION*. *Annual Review of Pharmacology and Toxicology*, 2004. **45**(1): p. 413-438.
58. Gebremedhin, D., et al., *Production of 20-HETE and Its Role in Autoregulation of Cerebral Blood Flow*. *Circulation Research*, 2000. **87**(1): p. 60-65.
59. Pearson, D.A., *Review of Clinical Guidelines for Cardiopulmonary Resuscitation*. *North Carolina Medical Journal*, 2015. **76**(4): p. 257-259.
60. Chen, L., et al., *20-HETE contributes to ischemia-induced angiogenesis*. *Vascular Pharmacology*.
61. Huang, H., M. Al-Shabrawey, and M.-H. Wang, *Cyclooxygenase- and cytochrome P450-derived eicosanoids in stroke*. *Prostaglandins & Other Lipid Mediators*, 2016. **122**: p. 45-53.
62. Spector, A.A. and H.-Y. Kim, *Cytochrome P450 epoxygenase pathway of polyunsaturated fatty acid metabolism*. *Biochimica et Biophysica Acta (BBA) - Molecular and Cell Biology of Lipids*, 2015. **1851**(4): p. 356-365.
63. Wu, S., et al., *Molecular Cloning and Expression of CYP2J2, a Human Cytochrome P450 Arachidonic Acid Epoxygenase Highly Expressed in Heart*. *Journal of Biological Chemistry*, 1996. **271**(7): p. 3460-3468.
64. Imig, J.D., et al., *Cytochrome P450 eicosanoids and cerebral vascular function*. *Expert Reviews in Molecular Medicine*, 2011. **13**: p. e7.
65. Spector, A.A., *Arachidonic acid cytochrome P450 epoxygenase pathway*. *Journal of Lipid Research*, 2009. **50**(Supplement): p. S52-S56.
66. Cazade, M., et al., *5,6-EET potently inhibits T-type calcium channels: implication in the regulation of the vascular tone*. *Pflügers Archiv - European Journal of Physiology*, 2013. **466**(9): p. 1759-1768.
67. Wang, Y., et al., *Arachidonic Acid Epoxygenase Metabolites Stimulate Endothelial Cell Growth and Angiogenesis via Mitogen-Activated Protein Kinase and Phosphatidylinositol 3-*

- Kinase/Akt Signaling Pathways*. Journal of Pharmacology and Experimental Therapeutics, 2005. **314**(2): p. 522-532.
68. Miksys, S.L. and R.F. Tyndale, *Drug-metabolizing cytochrome P450s in the brain*. Journal of Psychiatry and Neuroscience, 2002. **27**(6): p. 406-415.
  69. Qu, W., et al., *Cytochrome P450 CYP2J9, a New Mouse Arachidonic Acid  $\omega$ -1 Hydroxylase Predominantly Expressed in Brain*. Journal of Biological Chemistry, 2001. **276**(27): p. 25467-25479.
  70. Miller, T.M., et al., *Rapid, simultaneous quantitation of mono and dioxygenated metabolites of arachidonic acid in human CSF and rat brain*. Journal of Chromatography B, 2009. **877**(31): p. 3991-4000.
  71. Zhu, D., et al., *CYP4A mRNA, protein, and product in rat lungs: novel localization in vascular endothelium*. Journal of Applied Physiology, 2002. **93**(1): p. 330-337.
  72. MacVicar, B.A. and E.A. Newman, *Astrocyte Regulation of Blood Flow in the Brain*. Cold Spring Harbor Perspectives in Biology, 2015. **7**(5).
  73. Morisseau, C. and B.D. Hammock, *Impact of Soluble Epoxide Hydrolase and Epoxyeicosanoids on Human Health*. Annual review of pharmacology and toxicology, 2013. **53**: p. 37-58.
  74. Roman, R.J., et al., *Evidence that 20-HETE contributes to the development of acute and delayed cerebral vasospasm*. Neurological Research, 2006. **28**(7): p. 738-749.
  75. Alkayed, N.J., et al., *Inhibition of brain P-450 arachidonic acid epoxygenase decreases baseline cerebral blood flow*. American Journal of Physiology - Heart and Circulatory Physiology, 1996. **271**(4): p. H1541-H1546.
  76. Amruthesh, S.C., J.R. Falck, and E.F. Ellis, *Brain Synthesis and Cerebrovascular Action of Epoxygenase Metabolites of Arachidonic Acid*. Journal of Neurochemistry, 1992. **58**(2): p. 503-510.
  77. Iloff, J.J., et al., *A novel role for P450 eicosanoids in the neurogenic control of cerebral blood flow in the rat*. Exp Physiol, 2007. **92**(4): p. 653-8.
  78. Kehl, F., et al., *20-HETE contributes to the acute fall in cerebral blood flow after subarachnoid hemorrhage in the rat*. American Journal of Physiology - Heart and Circulatory Physiology, 2002. **282**(4): p. H1556-H1565.
  79. Miyata, N., et al., *Beneficial Effects of a New 20-Hydroxyeicosatetraenoic Acid Synthesis Inhibitor, TS-011 [N-(3-Chloro-4-morpholin-4-yl) Phenyl-N'-hydroxyimido Formamide], on Hemorrhagic and Ischemic Stroke*. Journal of Pharmacology and Experimental Therapeutics, 2005. **314**(1): p. 77-85.
  80. Takeuchi, K., et al., *Reversal of delayed vasospasm by an inhibitor of the synthesis of 20-HETE*. American Journal of Physiology - Heart and Circulatory Physiology, 2005. **289**(5): p. H2203-H2211.
  81. Poloyac, S.M., et al., *Identification and quantification of the hydroxyeicosatetraenoic acids, 20-HETE and 12-HETE, in the cerebrospinal fluid after subarachnoid hemorrhage*. Journal of Neuroscience Methods, 2005. **144**(2): p. 257-263.
  82. Crago, E.A., et al., *Cerebrospinal Fluid 20-HETE Is Associated With Delayed Cerebral Ischemia and Poor Outcomes After Aneurysmal Subarachnoid Hemorrhage*. Stroke, 2011. **42**(7): p. 1872-1877.
  83. Siler, D.A., et al., *Protective Role of P450 Epoxyeicosanoids in Subarachnoid Hemorrhage*. Neurocritical Care, 2014. **22**(2): p. 306-319.
  84. Donnelly, M.K., et al., *20-HETE is Associated with Unfavorable Outcomes in Subarachnoid*

- Hemorrhage Patients*. Journal of Cerebral Blood Flow & Metabolism, 2015. **35**(9): p. 1515-1522.
85. Martini, R.P., et al., *Genetic variation in soluble epoxide hydrolase is associated with outcome after aneurysmal subarachnoid hemorrhage*. Journal of neurosurgery, 2014. **121**(6): p. 1359-1366.
  86. Siler, D.A., et al., *Soluble Epoxide Hydrolase in Hydrocephalus, Cerebral Edema, and Vascular Inflammation After Subarachnoid Hemorrhage*. Stroke, 2015. **46**(7): p. 1916-1922.
  87. Poloyac, S.M., et al., *Protective Effect of the 20-HETE Inhibitor HET0016 on Brain Damage after Temporary Focal Ischemia*. Journal of Cerebral Blood Flow & Metabolism, 2006. **26**(12): p. 1551-1561.
  88. Tanaka, Y., et al., *Continuous inhibition of 20-HETE synthesis by TS-011 improves neurological and functional outcomes after transient focal cerebral ischemia in rats*. Neuroscience Research, 2007. **59**(4): p. 475-480.
  89. Ward, Natalie C., et al., *Cytochrome P450 metabolites of arachidonic acid are elevated in stroke patients compared with healthy controls*. Clinical Science, 2011. **121**(11): p. 501-507.
  90. Shaik, J.S.B., et al., *Soluble epoxide hydrolase inhibitor trans-4-[4-(3-adamantan-1-yl-ureido)-cyclohexyloxy]-benzoic acid is neuroprotective in rat model of ischemic stroke*. American Journal of Physiology - Heart and Circulatory Physiology, 2013. **305**(11): p. H1605-H1613.
  91. Zuloaga, K.L., et al., *Soluble epoxide hydrolase gene deletion improves blood flow and reduces infarct size after cerebral ischemia in reproductively senescent female mice*. Frontiers in Pharmacology, 2014. **5**: p. 290.
  92. Davis, C.M., et al., *Ultrasound stimulates formation and release of vasoactive compounds in brain endothelial cells*. American Journal of Physiology - Heart and Circulatory Physiology, 2015. **309**(4): p. H583-H591.
  93. Shaik, J.S.B., et al., *20-Hydroxyeicosatetraenoic Acid Inhibition by HET0016 Offers Neuroprotection, Decreases Edema, and Increases Cortical Cerebral Blood Flow in a Pediatric Asphyxial Cardiac Arrest Model in Rats*. Journal of Cerebral Blood Flow & Metabolism, 2015. **35**(11): p. 1757-1763.
  94. Zhu, J., et al., *Additive neuroprotection of a 20-HETE inhibitor with delayed therapeutic hypothermia after hypoxia-ischemia in neonatal piglets*. Developmental neuroscience, 2015. **37**(0): p. 376-389.
  95. Hutchens, M.P., et al., *Soluble epoxide hydrolase gene deletion reduces survival after cardiac arrest and cardiopulmonary resuscitation*. Resuscitation, 2008. **76**(1): p. 89-94.
  96. Wang, J., et al., *Inhibition of soluble epoxide hydrolase after cardiac arrest/cardiopulmonary resuscitation induces a neuroprotective phenotype in activated microglia and improves neuronal survival*. Journal of Cerebral Blood Flow & Metabolism, 2013. **33**(10): p. 1574-1581.
  97. Cumbler, E. and J. Glasheen, *Management of blood pressure after acute ischemic stroke: An evidence-based guide for the hospitalist*. Journal of Hospital Medicine, 2007. **2**(4): p. 261-267.
  98. Bederson, J.B., et al., *Guidelines for the Management of Aneurysmal Subarachnoid Hemorrhage: A Statement for Healthcare Professionals From a Special Writing Group of the Stroke Council, American Heart Association*. Stroke, 2009. **40**(3): p. 994-1025.
  99. Edson, K.Z. and A.E. Rettie, *CYP4 Enzymes As Potential Drug Targets: Focus on Enzyme Multiplicity, Inducers and Inhibitors, and Therapeutic Modulation of 20-*



- Hydroxyecosatetraenoic Acid (20-HETE) Synthase and Fatty Acid* #969;- Hydroxylase Activities. *Current Topics in Medicinal Chemistry*, 2013. **13**(12): p. 1429-1440.
100. Borrello, S., et al., *Restoration of hydroperoxide-dependent lipid peroxidation by 3-methylcholanthrene induction of cytochrome P-448 in hepatoma microsomes*. *FEBS Letters*, 1986. **209**(2): p. 305-310.
  101. Shak, S., et al., *Leukotriene B4 omega-hydroxylase in human polymorphonuclear leukocytes. Suicidal inactivation by acetylenic fatty acids*. *Journal of Biological Chemistry*, 1985. **260**(24): p. 13023-13028.
  102. Zou, A.P., et al., *Effects of 17-octadecynoic acid, a suicide-substrate inhibitor of cytochrome P450 fatty acid omega-hydroxylase, on renal function in rats*. *Journal of Pharmacology and Experimental Therapeutics*, 1994. **268**(1): p. 474-481.
  103. Ortiz de Montellano, P.R. and J.M. Mathews, *Autocatalytic alkylation of the cytochrome P-450 prosthetic haem group by 1-aminobenzotriazole. Isolation of an NN-bridged benzyne-protoporphyrin IX adduct*. *Biochemical Journal*, 1981. **195**(3): p. 761-764.
  104. Maier, K.G., et al., *Fluorescent HPLC assay for 20-HETE and other P-450 metabolites of arachidonic acid*. *American Journal of Physiology - Heart and Circulatory Physiology*, 2000. **279**(2): p. H863-H871.
  105. Sun, C.-W., et al., *Nitric Oxide-20-Hydroxyecosatetraenoic Acid Interaction in the Regulation of K<sup>+</sup> Channel Activity and Vascular Tone in Renal Arterioles*. *Circulation Research*, 1998. **83**(11): p. 1069-1079.
  106. Wang, M.-H., et al., *Cytochrome P450-Derived Arachidonic Acid Metabolism in the Rat Kidney: Characterization of Selective Inhibitors*. *Journal of Pharmacology and Experimental Therapeutics*, 1998. **284**(3): p. 966-973.
  107. Alonso-Galicia, M., et al., *Inhibition of 20-HETE Production Contributes to the Vascular Responses to Nitric Oxide*. *Hypertension*, 1997. **29**(1): p. 320-325.
  108. Miyata, N., et al., *HET0016, a potent and selective inhibitor of 20-HETE synthesizing enzyme*. *British Journal of Pharmacology*, 2001. **133**(3): p. 325-329.
  109. Mu, Y., et al., *Intravenous Formulation of HET0016 for Inhibition of Rat Brain 20-Hydroxyecosatetraenoic Acid (20-HETE) Formation*. *Drug metabolism and disposition: the biological fate of chemicals*, 2008. **36**(11): p. 2324-2330.
  110. Nakamura, T., et al., *Pyrazole and Isoxazole Derivatives as New, Potent, and Selective 20-Hydroxy-5,8,11,14-ecosatetraenoic Acid Synthase Inhibitors*. *Journal of Medicinal Chemistry*, 2003. **46**(25): p. 5416-5427.
  111. Lee, J.Y., et al., *Fluoxetine inhibits transient global ischemia-induced hippocampal neuronal death and memory impairment by preventing blood-brain barrier disruption*. *Neuropharmacology*, 2014. **79**: p. 161-171.
  112. Yuan, Z.-X. and S.I. Rapoport, *Transient postnatal fluoxetine decreases brain concentrations of 20-HETE and 15-epi-LXA4, arachidonic acid metabolites in adult mice*. *Prostaglandins, Leukotrienes and Essential Fatty Acids (PLEFA)*, 2015. **101**: p. 9-14.
  113. Poloyac, S.M., et al., *THE EFFECT OF ISONIAZID ON CYP2E1- AND CYP4A-MEDIATED HYDROXYLATION OF ARACHIDONIC ACID IN THE RAT LIVER AND KIDNEY*. *Drug Metabolism and Disposition*, 2004. **32**(7): p. 727-733.
  114. Elkhatali, S., et al., *19-Hydroxyecosatetraenoic acid and isoniazid protect against angiotensin II-induced cardiac hypertrophy*. *Toxicology and Applied Pharmacology*, 2015. **289**(3): p. 550-559.
  115. Wu, J.H.Y., et al., *Inhibition of 20-Hydroxyecosatetraenoic Acid Synthesis Using Specific*

- Plant Lignans: In Vitro and Human Studies*. Hypertension, 2009. **54**(5): p. 1151-1158.
116. Garcia, V., et al., *20-SOLA, a Novel Water Soluble 20-HETE Antagonist, Reduces Blood Pressure Through Regulation of Vascular ACE Expression via an IKK Dependent Pathway*. The FASEB Journal, 2015. **29**(1 Supplement).
  117. Kauser, K., et al., *Inhibitors of cytochrome P-450 attenuate the myogenic response of dog renal arcuate arteries*. Circulation Research, 1991. **68**(4): p. 1154-1163.
  118. Sato, M., et al., *Discovery of a N'-hydroxyphenylformamidine derivative HET0016 † as a potent and selective 20-HETE synthase inhibitor*. Bioorganic & Medicinal Chemistry Letters, 2001. **11**(23): p. 2993-2995.
  119. Sun, Q., et al., *1-Aminobenzotriazole, a Known Cytochrome P450 Inhibitor, Is a Substrate and Inhibitor of N-Acetyltransferase*. Drug Metabolism and Disposition, 2011. **39**(9): p. 1674-1679.
  120. CaJacob, C.A. and P.R. Ortiz de Montellano, *Mechanism-based in vivo inactivation of lauric acid hydroxylases*. Biochemistry, 1986. **25**(16): p. 4705-4711.
  121. Xu, F., et al., *Antihypertensive effect of mechanism-based inhibition of renal arachidonic acid  $\omega$ -hydroxylase activity*. American Journal of Physiology - Regulatory, Integrative and Comparative Physiology, 2002. **283**(3): p. R710-R720.
  122. Ramadan, E., et al., *Transient postnatal fluoxetine leads to decreased brain arachidonic acid metabolism and cytochrome P450 4A in adult mice*. Prostaglandins, Leukotrienes and Essential Fatty Acids (PLEFA), 2014. **90**(5): p. 191-197.
  123. Chang, T.K.H., J. Chen, and W.B.K. Lee, *Differential Inhibition and Inactivation of Human CYP1 Enzymes bytrans-Resveratrol: Evidence for Mechanism-Based Inactivation of CYP1A2*. Journal of Pharmacology and Experimental Therapeutics, 2001. **299**(3): p. 874-882.
  124. Elbarbry, F., A. Vermehren-Schmaedick, and A. Balkowiec, *Modulation of Arachidonic Acid Metabolism in the Rat Kidney by Sulforaphane: Implications for Regulation of Blood Pressure*. ISRN Pharmacology, 2014. **2014**: p. 683508.
  125. Bill, R.M., et al., *Overcoming barriers to membrane protein structure determination*. Nat Biotech, 2011. **29**(4): p. 335-340.
  126. Ubarretxena-Belandia, I. and D.L. Stokes, *Present and future of membrane protein structure determination by electron crystallography*. Advances in protein chemistry and structural biology, 2010. **81**: p. 33-60.
  127. Sánchez, R. and A. Šali, *Advances in comparative protein-structure modelling*. Current Opinion in Structural Biology, 1997. **7**(2): p. 206-214.
  128. Tianyun, L., W.T. Grace, and C. Emidio, *Comparative Modeling: The State of the Art and Protein Drug Target Structure Prediction*. Combinatorial Chemistry & High Throughput Screening, 2011. **14**(6): p. 532-547.
  129. Marti-Renom, M.A., B. Yerkovich, and A. Sali, *Comparative Protein Structure Prediction*, in *Current Protocols in Protein Science*. 2001, John Wiley & Sons, Inc.
  130. Altschul, S.F., et al., *Gapped BLAST and PSI-BLAST: a new generation of protein database search programs*. Nucleic Acids Research, 1997. **25**(17): p. 3389-3402.
  131. Taylor, W.R., T.P. Flores, and C.A. Orengo, *Multiple protein structure alignment*. Protein Science : A Publication of the Protein Society, 1994. **3**(10): p. 1858-1870.
  132. Kalsotra, A., et al., *Expression and characterization of human cytochrome P450 4F11: Putative role in the metabolism of therapeutic drugs and eicosanoids*. Toxicology and Applied Pharmacology, 2004. **199**(3): p. 295-304.

133. Chothia, C. and A.M. Lesk, *The relation between the divergence of sequence and structure in proteins*. The EMBO Journal, 1986. **5**(4): p. 823-826.
134. Vyas, V.K., et al., *Homology Modeling a Fast Tool for Drug Discovery: Current Perspectives*. Indian Journal of Pharmaceutical Sciences, 2012. **74**(1): p. 1-17.
135. Wallner, B. and A. Elofsson, *All are not equal: A benchmark of different homology modeling programs*. Protein Science : A Publication of the Protein Society, 2005. **14**(5): p. 1315-1327.
136. Larsson, P., et al., *Using multiple templates to improve quality of homology models in automated homology modeling*. Protein Science : A Publication of the Protein Society, 2008. **17**(6): p. 990-1002.
137. Rost, B., *Twilight zone of protein sequence alignments*. Protein Engineering, 1999. **12**(2): p. 85-94.
138. Petrey, D., et al., *Using multiple structure alignments, fast model building, and energetic analysis in fold recognition and homology modeling*. Proteins: Structure, Function, and Bioinformatics, 2003. **53**(S6): p. 430-435.
139. Xiang, Z., *Homology-Based Modeling of Protein Structure*, in *Computational Methods for Protein Structure Prediction and Modeling: Volume 1: Basic Characterization*, Y. Xu, D. Xu, and J. Liang, Editors. 2007, Springer New York: New York, NY. p. 319-357.
140. Vianna, C.P. and W.F. Azevedo, *Identification of new potential Mycobacterium tuberculosis shikimate kinase inhibitors through molecular docking simulations*. Journal of Molecular Modeling, 2011. **18**(2): p. 755-764.
141. Oprea, T.I. and H. Matter, *Integrating virtual screening in lead discovery*. Current Opinion in Chemical Biology, 2004. **8**(4): p. 349-358.
142. Schapira, M., et al., *In silico discovery of novel Retinoic Acid Receptor agonist structures*. BMC Structural Biology, 2001. **1**(1): p. 1-7.
143. Wermuth, C.G., et al., *Glossary of terms used in medicinal chemistry (IUPAC Recommendations 1998)*, in *Pure and Applied Chemistry*. 1998. p. 1129.
144. Yang, S.-Y., *Pharmacophore modeling and applications in drug discovery: challenges and recent advances*. Drug Discovery Today, 2010. **15**(11-12): p. 444-450.
145. Waltenberger, B., et al., *Discovery of Potent Soluble Epoxide Hydrolase (sEH) Inhibitors by Pharmacophore-Based Virtual Screening*. Journal of Chemical Information and Modeling, 2016. **56**(4): p. 747-762.
146. LeBrun, L.A., U. Hoch, and P.R. Ortiz de Montellano, *Autocatalytic Mechanism and Consequences of Covalent Heme Attachment in the Cytochrome P4504A Family*. Journal of Biological Chemistry, 2002. **277**(15): p. 12755-12761.
147. Hirani, V., et al., *EXPRESSION OF CYP4F2 IN HUMAN LIVER AND KIDNEY: ASSESSMENT USING TARGETED PEPTIDE ANTIBODIES*. Archives of biochemistry and biophysics, 2008. **478**(1): p. 59-68.
148. Zhou, S., *Cytochrome P450 2D6 : Structure, Function, Regulation and Polymorphism*. 2016, Boca Raton: CRC Press.
149. Sacerdoti, D., A. Gatta, and J.C. McGiff, *Role of cytochrome P450-dependent arachidonic acid metabolites in liver physiology and pathophysiology*. Prostaglandins & Other Lipid Mediators, 2003. **72**(1-2): p. 51-71.
150. Martignoni, M., G.M.M. Groothuis, and R. de Kanter, *Species differences between mouse, rat, dog, monkey and human CYP-mediated drug metabolism, inhibition and induction*. Expert Opinion on Drug Metabolism & Toxicology, 2006. **2**(6): p. 875-894.

151. Chauret, N., A. Gauthier, and D.A. Nicoll-Griffith, *Effect of Common Organic Solvents on in Vitro Cytochrome P450-Mediated Metabolic Activities in Human Liver Microsomes*. Drug Metabolism and Disposition, 1998. **26**(1): p. 1-4.
152. Shou, M., et al., *Activation of CYP3A4: Evidence for the Simultaneous Binding of Two Substrates in a Cytochrome P450 Active Site*. Biochemistry, 1994. **33**(21): p. 6450-6455.
153. Korzekwa, K.R., et al., *Evaluation of Atypical Cytochrome P450 Kinetics with Two-Substrate Models: Evidence That Multiple Substrates Can Simultaneously Bind to Cytochrome P450 Active Sites*. Biochemistry, 1998. **37**(12): p. 4137-4147.
154. Jin, R., et al., *Role of Human CYP4F2 in Hepatic Catabolism of the Proinflammatory Agent Leukotriene B4*. Archives of Biochemistry and Biophysics, 1998. **359**(1): p. 89-98.
155. McDonald, M.G., et al., *CYP4F2 Is a Vitamin K(1) Oxidase: An Explanation for Altered Warfarin Dose in Carriers of the V433M Variant*. Molecular Pharmacology, 2009. **75**(6): p. 1337-1346.
156. Liang, R., et al., *Influence of CYP4F2 genotype on warfarin dose requirement—a systematic review and meta-analysis*. Thrombosis Research, 2012. **130**(1): p. 38-44.
157. Jin, Y., et al., *CYP4F Enzymes Are Responsible for the Elimination of Fingolimod (FTY720), a Novel Treatment of Relapsing Multiple Sclerosis*. Drug Metabolism and Disposition, 2011. **39**(2): p. 191-198.
158. Sontag, T.J. and R.S. Parker, *Cytochrome P450  $\omega$ -Hydroxylase Pathway of Tocopherol Catabolism: NOVEL MECHANISM OF REGULATION OF VITAMIN E STATUS*. Journal of Biological Chemistry, 2002. **277**(28): p. 25290-25296.
159. Bardowell, S.A., D.E. Stec, and R.S. Parker, *Common Variants of Cytochrome P450 4F2 Exhibit Altered Vitamin E- $\omega$ -Hydroxylase Specific Activity*. The Journal of Nutrition, 2010. **140**(11): p. 1901-1906.
160. Michaels, S. and M.Z. Wang, *The Revised Human Liver Cytochrome P450 “Pie”: Absolute Protein Quantification of CYP4F and CYP3A Enzymes Using Targeted Quantitative Proteomics*. Drug Metabolism and Disposition, 2014. **42**(8): p. 1241-1251.
161. Lipinski, C.A., *Lead- and drug-like compounds: the rule-of-five revolution*. Drug Discovery Today: Technologies, 2004. **1**(4): p. 337-341.
162. Pajouhesh, H. and G.R. Lenz, *Medicinal Chemical Properties of Successful Central Nervous System Drugs*. NeuroRx, 2005. **2**(4): p. 541-553.
163. Simpkins, A.N., et al., *Soluble Epoxide Inhibition Is Protective Against Cerebral Ischemia via Vascular and Neural Protection*. The American Journal of Pathology. **174**(6): p. 2086-2095.
164. Luria, A., et al., *Compensatory Mechanism for Homeostatic Blood Pressure Regulation in Ephx2 Gene-disrupted Mice*. The Journal of biological chemistry, 2007. **282**(5): p. 2891-2898.
165. Li, L., et al., *Opposite Effects of Gene Deficiency and Pharmacological Inhibition of Soluble Epoxide Hydrolase on Cardiac Fibrosis*. PLoS ONE, 2014. **9**(4): p. e94092.